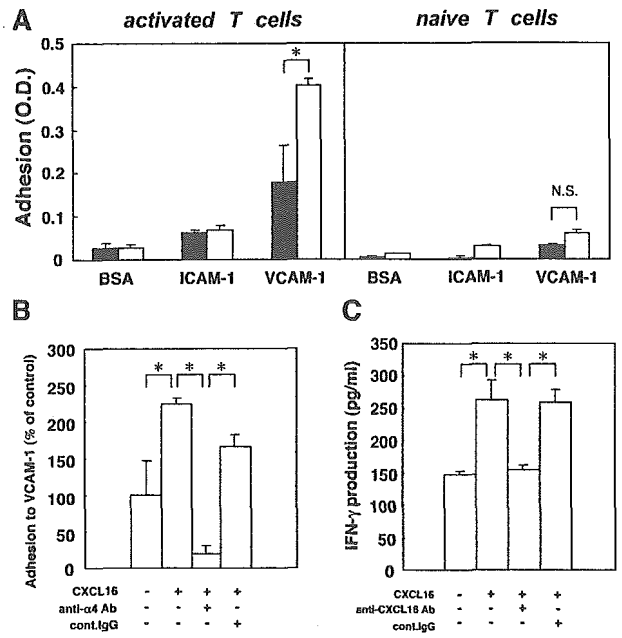

Figure 4. SR-PSOX/CXCL16 stimulated adhesion of activated $CD8^+$ T cells to VCAM-1 through activation of VLA-4 and enhanced IFN-γ production by activated $CD8^+$ T cells. A, Activated $CD8^+$ T cells were subjected to adhesion assays on heat-denatured BSA (as control), ICAM-1, or VCAM-1 for 10 minutes in the presence (open columns) or absence (closed columns) of 10 nM SR-PSOX/CXCL16. Data represent the mean±SD of triplicate measurements. Results are representative of two separate experiments (*$P<0.01$) (left panel). Naive $CD8^+$ T cells without activation were subjected to adhesion assays (right panel). B, Activated $CD8^+$ T cells were preincubated with 10 μg/mL anti-α4 antibody or control IgG (cont.IgG) for 1 hour. After incubation, cells were subjected to adhesion assays on VCAM-1 in the presence of 10 nM SR-PSOX/CXCL16 for 10 minutes. Data represent the mean±SD of triplicate measurements. Results are representative of two separate experiments (*:$P<0.01$). C, Activated $CD8^+$ T cells were co-cultured with either control CHO cells (CHO^-) or CHO cells with stable expression of SR-PSOX/CXCL16 (CXCL16), and INF-γ production was measured. For blocking experiments, activated $CD8^+$ T cells were preincubated with anti-SR-PSOX/CXCL16–neutralizing antibody (28 μg/mL) or control IgG (cont.IgG) for 1 hour. After preincubation, activated $CD8^+$ T cells were co-cultured with CHO cells expressing SR-PSOX/CXCL16 and IFN-γ production was measured. Data represent the mean±SD of quadricate measurements. (*:$P<0.01$). Ab indicates antibody.

Acknowledgments

We thank Noboru Ashida for his help in cell adhesion assay and Tomohiro Watanabe for his help in isolation of $CD8^+$ T cells. This work was supported by research grants from the MEXT of Japan (grants 13045019, 13832003, 15590738, 12CE2006, and13307034) and by a grant provided by the Ichiro Kanehara Foundation.

References

1. Rossi D, Zlotnik A. The biology of chemokines and their receptors. *Annu Rev Immunol.* 2000;18:217–242.
2. Mackay CR. Chemokines: immunology's high impact factors. *Nat Immunol.* 2001;2:95–101.
3. Luther SA, Cyster JG. Chemokines as regulators of T cell differentiation. *Nat Immunol.* 2001;2:102–107.
4. Strieter RM, Polverini PJ, Kunkel SL, Arenberg DA, Burdick MD, Kasper J, Dzuiba J, Van Damme J, Walz A, Marriott D, Chan SY, Roczniak S, Shanafelt AB. The functional role of the ELR motif in CXC chemokine-mediated angiogenesis. *J Biol Chem.* 1995;270:27348–27357.
5. Salcedo R, Young HA, Ponce ML, Ward JM, Kleinman HK, Murphy WJ, Oppenheim JJ. Eotaxin (CCL11) induces in vivo angiogenic responses by human $CCR3^+$ endothelial cells. *J Immunol.* 2001;166:7571–7578.
6. Baggiolini M. Chemokines and leukocyte traffic. *Nature.* 1998;392:565–568.
7. Moser B, Loetscher P. Lymphocyte traffic control by chemokines. *Nat Immunol.* 2001;2:123–128.
8. Sanchez-Madrid F, del Pozo MA. Leukocyte polarization in cell migration and immune interactions. *EMBO J.* 1999;18:501–511.
9. Gerszten RE, Garcia-Zepeda EA, Lim YC, Yoshida M, Ding HA, Gimbrone MA, Jr., Luster AD, Luscinskas FW, Rosenzweig A. MCP-1 and IL-8 trigger firm adhesion of monocytes to vascular endothelium under flow conditions. *Nature.* 1999;398:718–723.
10. Agace WW, Higgins JM, Sadasivan B, Brenner MB, Parker CM. T-lymphocyte-epithelial-cell interactions: integrin α(E)(CD103)β(7), LEEP-CAM and chemokines. *Curr Opin Cell Biol.* 2000;12:563–568.
11. Kunkel EJ, Butcher EC. Chemokines and the tissue-specific migration of lymphocytes. *Immunity.* 2002;16:1–4.
12. Matloubian M, David A, Engel S, Ryan JE, Cyster JG. A transmembrane CXC chemokine is a ligand for HIV-coreceptor Bonzo. *Nat Immunol.* 2000; 1:298–304.
13. Shimaoka T, Kume N, Minami M, Hayashida K, Kataoka H, Kita T, Yonehara S. Molecular cloning of a novel scavenger receptor for oxidized low density lipoprotein, SR-PSOX, on macrophages. *J Biol Chem.* 2000;275: 40663–40666.
14. Wilbanks A, Zondlo SC, Murphy K, Mak S, Soler D, Langdon P, Andrew DP, Wu L, Briskin M. Expression cloning of the STRL33/BONZO/ TYMSTR ligand reveals elements of CC, CXC, and CX3C chemokines. *J Immunol.* 2001;166:5145–5154.
15. Shimaoka T, Nakayama T, Kume N, Takahashi S, Yamaguchi J, Minami M, Hayashida K, Kita T, Ohsumi J, Yoshie O, Yonehara S. Cutting edge: SR-PSOX/CXC chemokine ligand 16 mediates bacterial phagocytosis by APCs through its chemokine domain. *J Immunol.* 2003;171:1647–1651.
16. Kruisbeek A. Preparation of cell suspensions from spleen, thymus and lymph node. In: Coligan JKA, Margulies D, Shewach EWS, eds. *Current Protocols in Immunology.* New York: Wiley; 1993.
17. Cycke N. Isolation of PP lymphocytes. In: Coligan JKA, Margulies D, Shewach EWS, eds. *Current Protocols in Immunology.* New York: Wiley; 1996.
18. Humphries MJ, Olden K, Yamada KM. A synthetic peptide from fibronectin inhibits experimental metastasis of murine melanoma cells. *Science.* 1986; 233:467–470.
19. Taooka Y, Chen J, Yednock T, Sheppard D. The integrin α9β1 mediates adhesion to activated endothelial cells and transendothelial neutrophil migration through interaction with vascular cell adhesion molecule-1. *J Cell Biol.* 1999;145:413–420.
20. Ashida N, Arai H, Yamasaki M, Kita T. Distinct signaling pathways for MCP-1-dependent integrin activation and chemotaxis. *J Biol Chem.* 2001; 276:16555–16560.
21. Mjaatvedt CH, Yamamura H, Wessels A, Ramsdell A, Turner D, Markwald R. Mechanisms of segmentation, septation, and remodeling of the tubular heart: endocardial cushion fate and cardiac looping. In: Harvey R, Rosenthal N, eds. *Heart Development.* San Diego: Academic Press; 1999.
22. Campbell JJ, Butcher EC. Chemokines in tissue-specific and microenvironment-specific lymphocyte homing. *Curr Opin Immunol.* 2000; 12:336–341.
23. Sallusto F, Lanzavecchia A, Mackay CR. Chemokines and chemokine receptors in T-cell priming and Th1/Th2-mediated responses. *Immunol Today.* 1998;19:568–574.
24. Hansson GK. Immune mechanisms in atherosclerosis. *Arterioscler Thromb Vasc Biol.* 2001;21:1876–1890.
25. Gor DO, Rose NR, Greenspan NS. TH1-TH2: a procrustean paradigm. *Nat Immunol.* 2003;4:503–505.
26. Friesel R, Komoriya A, Maciag T. Inhibition of endothelial cell proliferation by gamma-interferon. *J Cell Biol.* 1987;104:689–696.
27. Hansson GK, Hellstrand M, Rymo L, Rubbia L, Gabbiani G. Interferon gamma inhibits both proliferation and expression of differentiation-specific alpha-smooth muscle actin in arterial smooth muscle cells. *J Exp Med.* 1989;170:1595–1608.
28. Hansson GK, Holm J. Interferon-gamma inhibits arterial stenosis after injury. *Circulation.* 1991;84:1266–1272.
29. Cines DB, Pollak ES, Buck CA, Loscalzo J, Zimmerman GA, McEver RP, Pober JS, Wick TM, Konkle BA, Schwartz BS, Barnathan ES, McCrae KR, Hug BA, Schmidt AM, Stern DM. Endothelial cells in physiology and in the pathophysiology of vascular disorders. *Blood.* 1998;91:3527–3561.
30. Golbasi Z, Ucar O, Keles T, Sahin A, Cagli K, Camsari A, Diker E, Aydogdu S. Increased levels of high sensitive C-reactive protein in patients with chronic rheumatic valve disease: evidence of ongoing inflammation. *Eur J Heart Fail.* 2002;4:593–595.

Heidenhain Variant of Creutzfeldt-Jakob Disease: Diffusion-Weighted MRI and PET Characteristics

Yoshihisa Tsuji, MD
Hiroshi Kanamori, MD
Gaku Murakami, MD
Masayuki Yokode, MD
Takahiro Mezaki, MD
Katsumi Doh-ura, MD
Ken Taniguchi, MD
Kozo Matsubayashi, MD
Hidenao Fukuyama, MD
Toru Kita, MD
Makoto Tanaka, MD

ABSTRACT

Creutzfeldt-Jakob disease (CJD) is characterized by rapidly progressive dementia with a variety of neurological disorders and a fatal outcome. The authors present a case with visual disturbance as a leading symptom and rapid deterioration in global cognitive functions. The cerebrospinal fluid was positive for 14-3-3 protein, and diffusion-weighted magnetic resonance imaging (MRI) showed marked hyperintensity in the parieto-occipital cortices, where hypometabolism was clearly detected on positron emission tomography (PET). Pattern-reversal visual evoked potentials showed prolonged P100 latencies and increased N75/P100 amplitudes. All these findings supported a diagnosis of the Heidenhain variant of CJD, whereas a long clinical course, a lack of myoclonus, and an absence of periodic synchronous discharges on electroencephalography were atypical. Diffusion-weighted MRI and PET in combination with visual evoked potential recording and 14-3-3 protein detection may be useful for the early diagnosis of CJD.

Key words: Creutzfeldt-Jakob disease, visual disturbance, 14-3-3 protein, diffusion-weighted MRI, PET, visual evoked potentials.

Tsuji Y, Kanamori H, Murakami G, Yokode MD, Mezaki T, Doh-ura K, Taniguchi K, Matsubayashi K, Fukuyama H, Kita T, Makoto T. Heidenhain variant of Creutzfeldt-Jakob disease: diffusion-weighted MRI and PET characteristics. J Neuroimaging 2004;14:63-66.
DOI: 10.1177/1051228403258147

Creutzfeldt-Jakob disease (CJD) is a rare spongiform encephalopathy occurring sporadically in most cases. The diagnosis of CJD is based on clinical symptoms, such as rapidly progressive dementia, myoclonus, visual or cerebellar signs, pyramidal or extrapyramidal signs, and akinetic mutism, although the definite diagnosis of CJD requires pathological findings of the brain.[1] Periodic synchronous discharges (PSDs) on electroencephalography (EEG) and the detection of 14-3-3 protein in the cerebrospinal fluid (CSF) further support clinical suspicion of CJD.[1-4] Furthermore, magnetic resonance imaging (MRI), particularly diffusion-weighted imaging (DWI), has been shown to be useful in diagnosing the disease.[5-12] Herein, we report a probable case of CJD in which neuroimaging techniques proved useful in the early diagnosis of the disease. Progressive dementia, visual disturbance, 14-3-3 protein in the CSF, and neuroimaging findings supported a diagnosis of CJD, but other clinical manifestations were atypical, including a long clinical course, the absence of myoclonus, and no PSDs on EEG.

Case Presentation

A 54-year-old woman noticed blurred vision and visual metamorphosis in August 2001. Her visual disturbance worsened, and she gave up driving a car. At 2 months, her family noticed that she had memory impairment and disorientation for time and place. She often lost her way around her house. Her cognitive deterioration rapidly progressed, and she felt difficulties in

Received March 31, 2003, and in revised form May 6, 2003. Accepted for publication May 9, 2003.

From the Departments of Geriatric Medicine (YT, HK, GM, MT), Neurology (TM), Functional Brain Imaging, Human Brain Research Center (HF), and Cardiovascular Medicine (TK), Graduate School of Medicine, Kyoto University, Kyoto, Japan; the Translational Research Center, Faculty of Medicine, Kyoto University (MY); the Department of Neuropathology, Neurological Institute, Kyushu University, Kyushu, Japan (KD); the Department of Psychiatry, Shoraiso National Hospital (KT); and the Center for Southeast Asian Studies, Kyoto University (KM).

Address correspondence to Makoto Tanaka, MD, Department of Geriatric Medicine, Graduate School of Medicine, Kyoto University, 54 Shogoin-Kawahara-cho, Sakyo-ku, Kyoto 606-8507, Japan. E-mail: makoto@kuhp.kyoto-u.ac.jp.

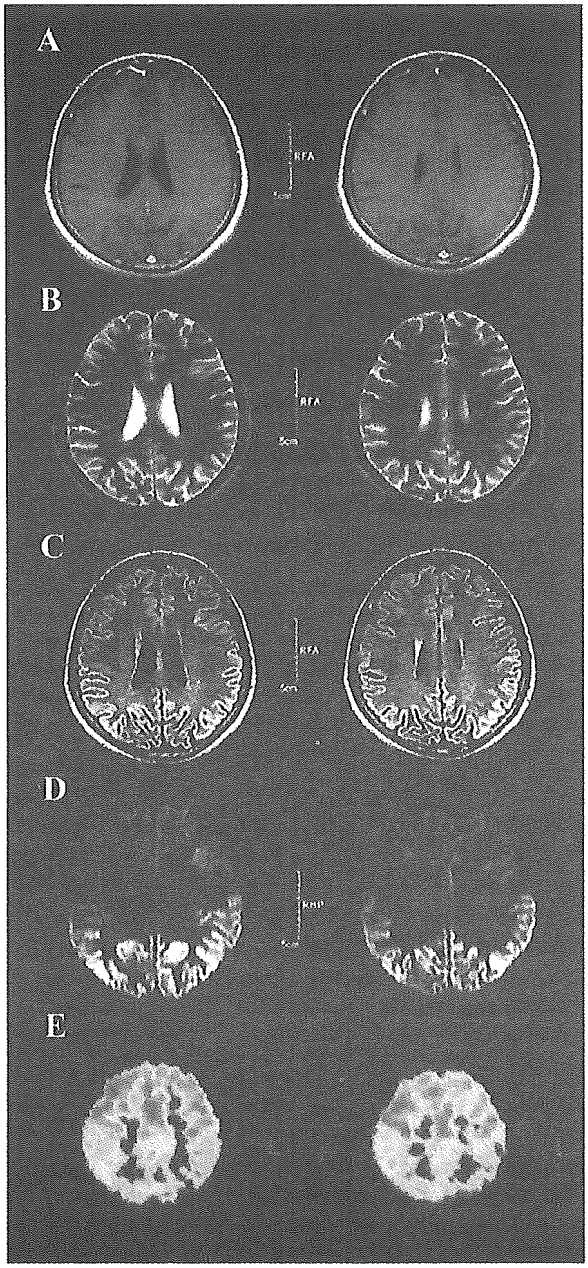

Fig 1. Magnetic resonance imaging (MRI) and positron emission tomography (PET) axial images. There was no atrophy, signs of cerebrovascular disease, or obvious signal abnormality on T1-weighted or T2-weighted MRI (A, B). High signal intensity in the parieto-occipital regions was detected on fluid-attenuated inversion recovery MRI (C), and the hyperintensity was most obvious on diffusion-weighted MRI (D). Low glucose metabolism was observed in the parieto-occipital regions as well as in the posterior cingulate cortex on PET (E). For the PET study, 5 mCi of [^{18}F]-fluorodeoxyglucose were administered intravenously, and scanning was performed using GE Advance (GE Medical Systems, Milwaukee, WI). Semiquantitative measurements were used.

calculation, reading, writing, and cooking at the beginning of 2002. She was often unable to locate the bathroom in her house by March 2002.

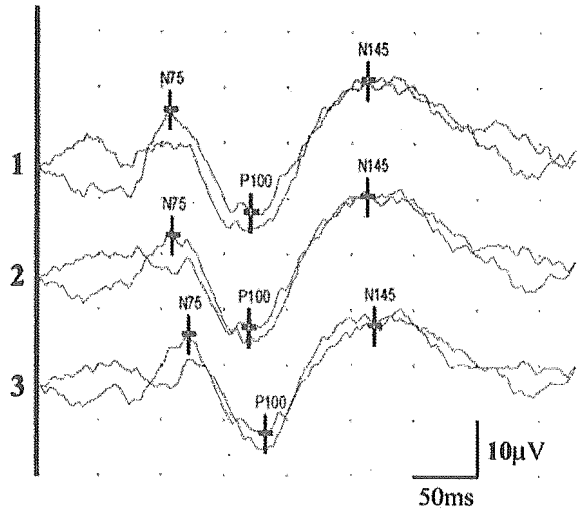

	Latency (ms)	Latency (ms)	Latency (ms)		Amplitude (μV)	Amplitude (μV)
1	N75 106	P100 170	N145 262		N75P100 18.75	P100N145 24.11
2	N75 108	P100 169	N145 262		N75P100 17.03	P100N145 24.27
3	N75 121	P100 182	N145 268		N75P100 18.38	P100N145 20.16

Fig 2. Pattern-reversal visual evoked potentials (VEPs). Binocular full-field pattern-reversal VEPs revealed prolonged P100 latencies and increased N75/P100 amplitudes. The active electrodes were placed on the left (1), the median (2), and the right (3) occipital scalp.

When she was admitted to Kyoto University Hospital in April 2002, she complained only of visual disturbance. Her medical history included operations for appendicitis and uterocervical cancer. There was no family history of dementia or psychiatric disease. She was not taking any regular medications. A neurological examination disclosed memory impairment, disorientation, anomia, alexia, agraphia, acalculia, dressing apraxia, color agnosia, and visual metamorphosis. A cranial nerve examination was normal. There were no pyramidal, extrapyramidal, or cerebellar signs or involuntary movements, including myoclonus. Her score on the Mini-Mental State Examination was 12 of 30, and she obtained a total IQ score of 48 on the Wechsler Adult Intelligence Scale–Revised.

The results of a blood test and a CSF examination were unremarkable except for positive 14-3-3 protein in the CSF. Lactic or pyruvic acid was not elevated in the CSF, and paraneoplastic markers, including anti-Hu and anti-Yo, were not detectable either in serum or in the CSF. Notably, an MRI examination revealed symmetric, bilateral, cortical hyperintensity in the parieto-occipital regions (Figs 1C, 1D). DWI most strikingly showed abnormalities in these areas (Fig 1D). There was no mass effect, atrophy, or signs of cerebrovascular disease (Figs 1A–1D). Moreover, positron emission tomography (PET) demonstrated metabolic disturbance in the parietal, occipital, and posterior cingulate cortices (Fig 1E). EEG showed diffuse slowing without typical PSDs. Pattern-reversal visual evoked potentials (VEPs) showed prolonged P100 latencies and increased N75/P100 amplitudes (normal P100 latency < 132 milliseconds,

normal N75/P100 amplitude < 10 μV[13]) (Fig 2). Genetic studies on the prion protein gene (PRNP) demonstrated no known mutations but disclosed homozygosity for methionine at the polymorphic codon 129. A brain biopsy could not be performed because we could not obtain permission from the patient's family.

At 16 months after the initial symptoms, limb and neck rigidity became apparent. At 20 months, she cannot recognize even her family members and has difficulty in oral communication because of the progression of agnosia and aphasia.

Discussion

Visual disturbance as a leading symptom, rapidly progressive dementia, and the detection of 14-3-3 protein in the CSF suggested a diagnosis of the Heidenhain variant of CJD.[14] Methionine homozygosity at codon 129 of the PRNP gene was consistent with this subtype.[15] However, this case did not fulfill the criteria for even possible CJD until the patient exhibited pronounced rigidity at 16 months after the initial symptoms.[1] This was due to the lack of some common clinical manifestations of CJD in this patient, including myoclonus, ataxia, and PSDs on EEG. This case not only suggests a heterogeneity of clinical presentation among patients with CJD but indicates difficulty in the early diagnosis of CJD without typical presentation. Currently used diagnostic criteria based on clinical symptoms and EEG findings may miss some CJD cases without typical sets of clinical manifestations, as in this case. Therefore, it is important to use neuroimaging and laboratory examinations for the early diagnosis of the disease.

Increased T2-weighted MRI signal has been described in the basal ganglia,[5,8] and recently, cortical hyperintensity was shown on diffusion-weighted MRI in some CJD cases with typical clinical courses.[6,7,10,11,16] Moreover, areas of signal abnormalities on diffusion-weighted MRI were well correlated with the neuropathologic findings of spongiform encephalopathy.[10] In the present case, hyperintensity in the parieto-occipital lobes was clearly shown on diffusion-weighted MRI early in the clinical course, indicating that diffusion-weighted MRI is useful for the early diagnosis of CJD.

There has been a relatively limited number of reports describing PET studies of CJD.[6,17,18] Henkel et al[18] analyzed PET studies of 8 patients with CJD and found decreased glucose metabolism in the occipital lobe, cerebellum, or basal ganglia in addition to temporal or parietal cortical region. In the preset case, metabolic disturbance was observed in the parietal, occipital, and posterior cingulate cortices. Although metabolic reductions in the parietal and posterior cingulate cortices are seen in other dementing diseases,[19,20] the clear involvement of the occipital lobes differed from the typical pattern of disturbance detected in Alzheimer's disease,[20] which is the most frequent misdiagnosis of CJD.[21] It may be more difficult to distinguish dementia with Lewy bodies (DLB) from CJD on PET, because significant metabolic reductions in the occipital cortex can be also seen in DLB.[20,22] Diffusion-weighted MRI and 14-3-3 protein detection may be useful in the differential diagnosis of the 2 diseases.[23]

VEPs may also provide a diagnostic aid for the early detection of CJD. According to previous reports, P100 latencies were increased or normal, but increased P100 amplitudes were the most frequent finding in CJD patients, particularly during the early stages of the disease.[13,24,25] Our case also showed increased P100 amplitudes at the early phase of the disease, thus indicating that VEP recording may be helpful, particularly in the early diagnosis of CJD without typical clinical presentation.

14-3-3 protein is expressed in all eukaryotic cells and participates in the regulation of diverse biological processes, including neuronal development, cell growth control, and cell cycling. There are 7 isoforms, 5 of which are present in neuronal cells and constitute nearly 1% of all soluble brain proteins.[26] The detection of 14-3-3 protein in the CSF probably reflects severe neuronal destruction.[23] 14-3-3 protein in the CSF has been shown to be a useful biochemical marker for CJD,[2,4] and Zerr et al[4] demonstrated that the specificity was even higher than that of PSDs on EEG. In the recent revised version of the French and European study criteria, positive 14-3-3 protein detection is considered as a criterion equivalent to a typical EEG.[1] According to the revised version, our patient was classified as probable CJD.

CJD may be a more heterogeneous group of disorders than has been recognized, and neuroimaging techniques, including diffusion-weighted MRI and PET, in combination with VEPs and 14-3-3 protein detection may be useful for the early diagnosis of CJD.

References

1. Brandel JP, Delasnerie-Laupretre N, Laplanche JL, Hauw JJ, Alperovitch A. Diagnosis of Creutzfeldt-Jakob disease: effect of clinical criteria on incidence estimates. *Neurology* 2000;54:1095-1099.
2. Hsich G, Kenney K, Gibbs CJ, Lee KH, Harrington MG. The 14-3-3 brain protein in cerebrospinal fluid as a marker for transmissible spongiform encephalopathies. *N Engl J Med* 1996;335:924-930.
3. Staffen W, Trinka E, Iglseder B, Pilz P, Homann N, Ladurner G. Clinical and diagnostic findings in a patient with Creutzfeldt-Jakob disease (type Heidenhain). *J Neuroimaging* 1997;7:50-54.
4. Zerr I, Pocchiari M, Collins S, et al. Analysis of EEG and CSF 14-3-3 proteins as aids to the diagnosis of Creutzfeldt-Jakob disease. *Neurology* 2000;55:811-815.
5. Finkenstaedt M, Szudra A, Zerr I, et al. MR imaging of Creutzfeldt-Jakob disease. *Radiology* 1996;199:793-798.
6. Na DL, Suh CK, Choi SH, et al. Diffusion-weighted magnetic resonance imaging in probable Creutzfeldt-Jakob disease: a clinical-anatomic correlation. *Arch Neurol* 1999; 56:951-957.
7. Demaerel P, Heiner L, Robberecht W, Sciot R, Wilms G. Diffusion-weighted MRI in sporadic Creutzfeldt-Jakob disease. *Neurology* 1999;52:205-208.
8. Schroter A, Zerr I, Henkel K, Tschampa HJ, Finkenstaedt M, Poser S. Magnetic resonance imaging in the clinical diagnosis of Creutzfeldt-Jakob disease. *Arch Neurol* 2000;57: 1751-1757.
9. Jacobs DA, Lesser RL, Mourelatos Z, Galetta SL, Balcer LJ. The Heidenhain variant of Creutzfeldt-Jakob disease: clinical, pathologic, and neuroimaging findings. *J Neuroophthalmol* 2001;21:99-102.
10. Mittal S, Farmer P, Kalina P, Kingsley PB, Halperin J. Correlation of diffusion-weighted magnetic resonance imaging with neuropathology in Creutzfeldt-Jakob disease. *Arch Neurol* 2002;59:128-134.

11. Rabinstein AA, Whiteman ML, Shebert RT. Abnormal diffusion-weighted magnetic resonance imaging in Creutzfeldt-Jakob disease following corneal transplantations. *Arch Neurol* 2002;59:637-639.
12. Eschweiler GW, Wormstall H, Widmann U, Naegele T, Bartels M. Correlation of diffusion-weighted magnetic resonance imaging with neurological deficits in sporadic Creutzfeldt-Jakob Disease. *Nervenarzt* 2002;73:883-886.
13. de Seze J, Hache JC, Vermersch P, et al. Creutzfeldt-Jakob disease: neurophysiologic visual impairments. *Neurology* 1998;51:962-967.
14. Kropp S, Schulz-Schaeffer WJ, Finkenstaedt M, et al. The Heidenhain variant of Creutzfeldt-Jakob disease. *Arch Neurol* 1999;56:55-61.
15. Parchi P, Giese A, Capellari S, et al. Classification of sporadic Creutzfeldt-Jakob disease based on molecular and phenotypic analysis of 300 subjects. *Ann Neurol* 1999;46: 224-233.
16. Bahn MM, Parchi P. Abnormal diffusion-weighted magnetic resonance images in Creutzfeldt-Jakob disease. *Arch Neurol* 1999;56:577-583.
17. Grunwald F, Pohl C, Bender H, et al. 18F-fluorodeoxyglucose-PET and 99mTc-bicisate-SPECT in Creutzfeldt-Jakob disease. *Ann Nucl Med* 1996;10:131-134.
18. Henkel K, Zerr I, Hertel A, et al. Positron emission tomography with [(18)F]FDG in the diagnosis of Creutzfeldt-Jakob disease (CJD). *J Neurol* 2002;249:699-705.
19. Minoshima S, Giordani B, Berent S, Frey KA, Foster NL, Kuhl DE. Metabolic reduction in the posterior cingulate cortex in very early Alzheimer's disease. *Ann Neurol* 1997; 42:85-94.
20. Minoshima S, Foster NL, Sima AA, Frey KA, Albin RL, Kuhl DE. Alzheimer's disease versus dementia with Lewy bodies: cerebral metabolic distinction with autopsy confirmation. *Ann Neurol* 2001;50:358-365.
21. Poser S, Mollenhauer B, Kraubeta A, et al. How to improve the clinical diagnosis of Creutzfeldt-Jakob disease. *Brain* 1999;122:2345-2351.
22. Lobotesis K, Fenwick JD, Phipps A, et al. Occipital hypoperfusion on SPECT in dementia with Lewy bodies but not AD. *Neurology* 2001;56:643-649.
23. Haik S, Brandel JP, Sazdovitch V, et al. Dementia with Lewy bodies in a neuropathologic series of suspected Creutzfeldt-Jakob disease. *Neurology* 2000;55:1401-1404.
24. Aguglia U, Farnarier G, Regis H, Oliveri RL, Quattrone A. Sensory evoked potentials in Creutzfeldt-Jakob disease. *Eur Neurol* 1990;30:157-161.
25. Finsterer J, Bancher C, Mamoli B. Giant visually-evoked potentials without myoclonus in the Heidenhain type of Creutzfeld-Jakob disease. *J Neurol Sci* 1999;167:73-75.
26. Green AJ. Use of 14-3-3 in the diagnosis of Creutzfeldt-Jakob disease. *Biochem Soc Trans* 2002;30:382-386.

THE JOURNAL OF BIOLOGICAL CHEMISTRY
Vol. 279, No. 14, Issue of April 2, pp. 14201–14206, 2004
Printed in U.S.A.

Type IV Collagen Is Transcriptionally Regulated by Smad1 under Advanced Glycation End Product (AGE) Stimulation*

Received for publication, September 22, 2003, and in revised form, January 15, 2004
Published, JBC Papers in Press, January 19, 2004, DOI 10.1074/jbc.M310427200

Hideharu Abe‡, Takeshi Matsubara§, Noriyuki Iehara¶, Kojiro Nagai§, Toshikazu Takahashi‡, Hidenori Arai§, Toru Kita‖, Toshio Doi‡**

From the ‡Department of Clinical Biology and Medicine, Course of Biological Medicine, University of Tokushima, Tokushima 770-8503, Japan and the Departments of §Geriatric Medicine, ¶Artificial Kidney, and ‖Cardiovascular Medicine, Kyoto University Graduate School of Medicine, Kyoto 606-8507, Japan

Prolonged exposure to hyperglycemia is now recognized as the most significant causal factor of diabetic complications. Excessive advanced glycation end products (AGEs) as a result of hyperglycemia in tissues or in the circulation may critically affect the progression of diabetic nephropathy. In diabetic nephropathy, glomerulosclerosis is a typical pathologic feature characterized by the increase of the extracellular matrix (ECM). We have reported previously that α1 type IV collagen (Col4) is one of the major components of ECM, which is up-regulated by AGEs, and that the overexpression of Col4 is transcriptionally regulated by an unknown transcription factor binding to the promoter. Here we identified this protein as Smad1 by yeast one-hybrid screening. Using chromatin immunoprecipitation and reporter assay, we observed that Smad1 directly regulated transcription for Col4 through the binding of Smad1 to the promoter of Col4. Smad1 was significantly induced along with Col4 in AGE-treated mesangial cells. Moreover, suppression of Smad1 by antisense morpholino resulted in a decrease of AGE-induced Col4 overproduction. To elucidate the interaction between transforming growth factor-β and Smad1, we investigated whether activin receptor-liked kinase1 (ALK1) was involved in this regulation. AGE stimulation significantly increased the expression of the ALK1 mRNA in mesangial cells. We also demonstrated that Smad1 and ALK1 were highly expressed in human diabetic nephropathy. These results suggest that the modulation of Smad1 expression is responsible for the initiation and progression of diabetic nephropathy and that blocking Smad1 signaling may be beneficial in preventing diabetic nephropathy and other various diabetic complications.

Diabetic nephropathy is the leading cause of end-stage renal disease and a major contributing cause of morbidity and mortality in patients with diabetes throughout the world. There is accumulating evidence that AGEs[1] have a pathogenic role in the development of diabetic glomerulosclerosis. Excessive AGEs produced as the result of hyperglycemia are known to stimulate the production of the ECM and inhibits its degradation. AGEs have a wide range of chemical, cellular, and tissue effects through changes in charge, solubility, and conformation that characterize molecular senescence. AGEs induce a variety of cellular events in vascular cells and other cells, possibly through several functional AGE receptors, thereby modulating the disease processes (1–5). AGEs have recently been accepted as having an important role, not only in diabetic complications but also in aging and old age-related diseases, including atherosclerosis (6, 7). Moreover, a truncated, soluble form of the receptor for AGEs was reported to suppress the development of accelerated diabetic atherosclerosis (8). Exposure of cultured mesangial cells to AGEs results in a receptor-mediated up-regulation of mRNA and protein secretion of Col4 (5, 9). However, there is little information regarding the mechanisms that underlie this regulation.

It was recently shown that TGF-β plays an important role in the AGE response of the glomeruli (10). Transgenic mice overexpressing TGF-β develop severe glomerulosclerosis (11). Thus, TGF-β is a central mediator of the sclerosing process in diabetic nephropathy. Members of the TGF-β superfamily bind to two different types of serine/threonine kinase receptors, termed type I and type II receptors (12). Type II receptors activate type I receptors, and signals are mediated through the type I receptors. Ligand-specific Smads are direct substrates of type I receptor kinases. Thus, the specificity of the signals is determined by type I receptors. ALK1 is one of the type I receptor members for TGF-β family proteins and has been linked to the inherited multisystemic vascular disorder, hereditary hemorrhagic telangiectasia 2 (HHT2). Although ALK1 has been known as an orphan receptor, recent reports show that ALK1 transduces TGF-β signals via Smad1 (13, 14).

Morphologically, the development of diabetic nephropathy is characterized by progressive thickening of the glomerular basement membrane (GBM) and, by expansion, of the mesangial ECM. During the process of glomerular injuries, mesangial cells can overproduce Col4 and secrete type I collagen (Col1) and osteopontin (OPN), which are not normally present in the mesangial matrix (15). In particular, Col4 is a major component of the thickened GBM and expanded ECM, but no molecules that directly regulate the Col4 expression have been found. The 130-bp bidirectional promoter of Col4 contains a large stem-loop structure (CIV), which has been shown to interact with several DNA-binding proteins (16). Using a gel mobility shift assay, we reported previously that an unknown protein binding to the CIV site directly regulates Col4 expression only when exposed to AGEs (9). To identify the protein

* This work was supported by Grant-in Aid from the Ministry of Education, Science, Sports and Culture of Japan. The costs of publication of this article were defrayed in part by the payment of page charges. This article must therefore be hereby marked "*advertisement*" in accordance with 18 U.S.C. Section 1734 solely to indicate this fact.

** To whom correspondence should be addressed. Tel.: 81-88-633-7184; Fax: 81-88-633-9245; E-mail: doi@clin.med.tokushima-u.ac.jp.

[1] The abbreviations used are: AGE, advanced glycation end product; ALK1, activin receptor-liked kinase1; AS, antisense; BMP, bone morphogenetic protein; BSA, bovine serum albumin; Col1, type I collagen; Col4, α1 type IV collagen; ECM, extracellular matrix; GBM, glomerular basement membrane; OPN, osteopontin; pSmad1, phosphorylated Smad1; TGF, transforming growth factor

that binds to the CIV site in the promoter region of the mouse *Col4* gene, we constructed a cDNA library from mouse mesangial cells treated with AGEs. In this study, we used a yeast one-hybrid system to isolate a clone that encodes a specific transcription factor from the library, and we identified the clone as the cDNA that encodes Smad1.

EXPERIMENTAL PROCEDURES

Cell Culture—A glomerular mesangial cell line was established from glomeruli isolated from normal, 4-week-old mice (C57BL/6JxSJL/J) and was identified according to the method described previously (17). The mesangial cells were maintained in B medium (a 3:1 mixture of minimal essential medium/F12 modified with trace elements) supplemented with 1 mM glutamine, penicillin at 100 units/ml, streptomycin at 100 mg/ml, and 20% fetal calf serum. The cultured cells fulfilled the criteria generally accepted for glomerular mesangial cells previously (17). AGE or bovine serum albumin (BSA) exposure was carried out as described previously (9).

Preparation of AGEs—AGE-BSA was prepared by incubating BSA in phosphate-buffered saline (10 mM, pH 7.4) with 50 mM glucose 6-phosphate for 8 weeks at 37 °C as described previously (5). Unmodified BSA was incubated under the same conditions without glucose 6-phosphate as control. Protein concentrations were measured by the Bradford method. All AGE-protein specific fluorescence intensities were measured at a protein concentration of 1 mg/ml. AGE-BSA and control BSA contained 61.3 and 8.31 units of AGE per milligram of protein, respectively.

cDNA Library Construction and Yeast One-hybrid Screening—We prepared cDNA from mouse mesangial cells exposed to AGEs and inserted it into the pGAD10 vector. Yeast one-hybrid screening was carried out according to the MATCHMAKER one-hybrid protocol (Clontech). Briefly, tandem repeats of the 27-bp sequence (5′-TTCCTCCCCTTGGAGGAGCGCCGCCCG-3′; CIV-1) from the mouse type IV collagen gene were ligated into the yeast integration and reporter vector pHISi or pLacZi to generate pHISi-CIV-1 or pLacZi-CIV-1, respectively (18). Each pHISi-CIV-1 and pLacZi-CIV-1 reporter construct was linearized and integrated into the genome of competent yeast YM4271, sequentially. The resulting yeast cells with the integrated pHISi-CIV-1 and pLacZi-CIV-1 were used for one-hybrid screening with the AGE-stimulated mouse mesangial cell library. Positive colonies were selected on synthetic dropout −His/−Leu plates with 45 mM 3-amino-1, 2, 4-triazole (3-AT). To exclude false positive clones, we performed a β-galactosidase filter lift assay according to manufacturer's instructions (Clontech). Plasmids were rescued from selected blue yeast colonies and retransformed into *E. coli* DH5α.

Chromatin Immunoprecipitation Assay—Chromatin immunoprecipitation assays were performed essentially as described previously by Luo *et al.* (19). We used anti-Smad1 antibody, anti-Smad4 antibody (Santa Cruz Biotechnology), or normal control IgG at 4 °C overnight. PCR was performed with primers to amplify the region containing the CIV-1 motif. The 5′-primer was 5′-GGAGCTCCCCAATTTGTTG-3′, and the 3′ primer was 5′-CAGCCTCCGCCTCTTACC-3′. The resulting product was ~100 bp by agarose gel electrophoresis.

Reporter Assay—1.3 × 10^5 COS7 cells in 10% fetal bovine serum/Dulbecco's modified Eagle's medium were seeded into 6-well plates. Eight hours later, the cells were transfected with 750 ng of CIV-1-LacZ reporter construct along with either 750 ng of vector encoding wild type Smad1 or the mock vector and 75 ng of CMV-LUC (Firefly luciferase under the control of cytomegalovirus promoter) as an internal control. Transfection was performed with FuGENE6 transfection reagent (Roche Molecular Biochemicals) according to the manufacturer's instructions. Forty-eight hours later, the cells were harvested in reporter lysis buffer, and β-galactosidase and luciferase activities were then measured using the Luminescent β-galactosidase reporter system (BD Biosciences) and the luciferase reporter assay system from Promega. β-galactosidase results were normalized for luciferase activity.

RNase Protection Assay—Total RNA was isolated from mesangial cells using the TRIsol reagent (Invitrogen), and an RNase protection assay was performed as described previously (20). Briefly, the RNA probes were prepared by linearizing the PvuII fragment of Col4 from p1234, the ApaI fragment of Col1 from pGM101, and the EcoRI fragment of glyceraldehyde-3-phosphate dehydrogenase (GAPDH) from pMGAP1. In addition, mouse riboprobe for Smad1 (5′-GCAAGTTTTGCGATGTGAGA-3′ and 5′-GCATCTTCCAGAGTGAAGCC-3′), ALK1 (5′-GAGTGTGGCGGTCAAGATTT-3′ and 5′-GGAGCCGTGTTCATGGTAGT-3′), and osteopontin (5′-TGCACCCAGATCCTATAGCC-3′ and 5′-CCTCAGTCCATAAGCCAAGC-3′) were amplified by reverse transcription PCR. The PCR fragments were sequenced to confirm that they were the respective cDNAs and then were cloned into a pGEM-T plasmid. After digesting the plasmid with SacI, an antisense riboprobe was synthesized *in vitro* using T7 RNA polymerase. The RNA probes and the test RNA were hybridized overnight at 45 °C. RNase A (40 μg/ml) and RNase T1 (2 μg/ml) were added to each tube, and the tubes were incubated for 1 h at 30 °C. The RNase resistant fragments were analyzed by 5% polyacrylamide/8 M urea gel electrophoresis and autoradiography. The protected bands for each RNA probe had the same size as the coding sequence for the specific mRNA, thus providing evidence for their specificity, and were evaluated by densitometric analysis.

Western Blotting—Cultured mesangial cells were treated with AGEs or BSA for 72 h. Cells were harvested in sample buffer, resolved by SDS-polyacrylamide gel electrophoresis, transferred to nitro-cellulose membrane, subjected to Western blot using a 1:500 dilution of antibody for Smad1 and pSmad1 (Santa Cruz Biotechnology), and detected using an enhanced chemiluminescence detection system (Invitrogen).

Immunostaining of Cultured Cells—Cultured cells were fixed in 4% paraformaldehyde. The antibodies used were anti-Smad1 antibody, 1:100 (Santa Cruz Biotechnology), and anti-pSmad1, 1:100 (Calbiochem). An appropriate fluorescein isothiocyanate-conjugated secondary antibody was used for visualization, and imaging was done using a confocal laser microscope and a fluorescent microscope (Olympus).

Smad1 Morpholino Antisense Oligonucleotide—The antisense oligonucleotide used was a 25-nucleotide morpholino oligo (Genetools LLC) with the base composition 5′-CAAGCTGGTCACATTCATAGCGGCT-3′. A standard morpholino oligo with the base composition 5′-CAtGCTcGTCACATTCAaAGCcGCT-3′ (points of mismatch are shown by small letters) was used as a control. Microinjection of *in vitro* transcribed RNA was performed as described previously (21).

Histology—Histopathological studies were performed on human tissues. This study was in accordance with the Declaration of Helsinki, and we obtained approval from the institutional review board. All patients gave their informed written consent. Diabetic kidney specimens (n = 5) were obtained from renal biopsies. Control human tissue sections were obtained from normal renal cortex harvested from kidneys removed for renal malignancy. Tissues for analysis were sampled from the pole opposite the tumor. Cryopreserved kidney tissues were cut in 5-μm-thick sections and fixed in acetone for 5 min. Endogenous peroxidase activity was quenched by a 20-min incubation in the dark with 1% H_2O_2 in methanol. To eliminate nonspecific staining, sections were incubated with the appropriate preimmune serum for 20 min at room temperature, followed by incubation with primary antibodies anti-Smad1 (Santa Cruz Biotechnology) and anti-ALK1 (R&D Systems) antibodies.

RESULTS

Smad1 Is Identified as a Binding Protein to Col4—To identify the protein binds to the CIV site in the promoter region of the mouse *Col4* gene, we constructed a cDNA library from mouse mesangial cells treated with AGEs. We then used a yeast one-hybrid system to isolate a clone that encodes a specific transcription factor from the library. We identified this clone as the cDNA that encodes Smad1. Smad1 is well known for transducing the bone morphogenetic protein (BMP) signal (22) and is essentially important in the development of kidney (23). However, the expression of Smad1 is not detected in glomeruli in adult mouse (24).

To confirm the binding of Smad1 to the *Col4* promoter *in vivo*, we performed a chromatin immunoprecipitation assay. Precipitated DNA was purified, and the promoter of the *Col4* gene was detected by PCR. The anti-Smad1 antibody precipitated chromatin containing the CIV-1 site from cells stimulated with AGEs (Fig. 1). In contrast, considerably less binding was observed in BSA-exposed cells. We also detected Smad4 on the CIV-1 site (Fig. 1). These observations suggest that Smad1 and Smad4 can target the CIV motif in mesangial cells, especially when exposed to AGEs.

Smad1 Transcriptionally Regulates Col4 Expression—Next, we examined the transcriptional activity of the *Col4* gene by a reporter assay. We constructed a vector by fusing the *CIV-1* promoter in front of the LacZ reporter and then cotransfected

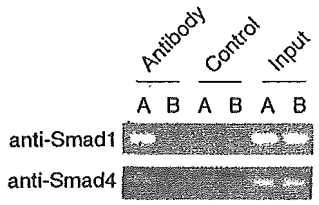

FIG. 1. **Binding of Smad1 to *Col4* promoter.** Chromatin immunoprecipitation was carried out with mesangial cells under treatment with AGEs (*A*) or BSA (*B*) using the indicated antibodies. PCR was performed using primers for the CIV-1 motif. After sonication, DNA from 10% of each sample was saved as input fraction (*Input*). One of three independent experiments is shown.

with a wild-type Smad1 vector in COS7 cells. First, we confirmed the expression of Smad1 by Western blot analysis (Fig. 2*a*). Phosphorylated Smad1 (pSmad1) was detected in cell lysates that had been tranfected with wild-type Smad1 vector. Cotransfection of the wild-type Smad1 resulted in an 18-fold increase in a relative β-galactosidase activity of Col4 compared with that of the vector alone (Fig. 2*b*, *mock*). The *CIV-1* promoter has a GC-rich sequence in its 3′ end, which has been identified as a binding site for Smad1 (25). We then constructed two mutant reporter plasmids, the deletion mutant of GC rich in CIV-1 (5′-TTCCTCCCCTTGGAGGA-3′; Mut1) and the trinucleotide substitution mutant of GC rich motif in CIV-1 (5′-TTCCTCCCCTTGGAGGAGCaCtGtCCG-3′; Mut2) (points of mutation are shown by small, underlined letters). The promoter activities of Mut1 and Mut2 were reduced to 4.9- and 4.3-fold increase, respectively (data not shown). β-galactosidase activity was normalized to luciferase activity and standardized as fold changes relative to cells cotransfected with the mock vector. In contrast, mock had no effect on the β-galactosidase activity in cotransfected cells. These results suggest that Smad1 is significantly involved in the induction of *Col4* gene transcription.

Activation and Translocation of Smad1 under AGE Exposure—To determine whether Smad1 is transcriptionally up-regulated by AGEs, we examined the expression of Smad1 in mesangial cells with or without AGEs stimulation. The levels of Smad1 mRNA were proportionally increased in a time-dependent manner (Fig. 3*a*). Similarly, the levels of *Col4* mRNA increased in parallel with the up-regulation of Smad1 transcripts. After BSA treatment, however, no change in the mRNA expression of *Smad1* or *Col4* was detected. Smad1 is well known to be phosphorylated and translocated into the nucleus, where it participates in the transcriptional regulation of target genes (22, 26). Therefore, we next examined the issue of whether the phosphorylation and translocation of Smad1 is affected by AGE treatment in mesangial cells (Fig. 3*b*). Consistent with the RNase protection assay, Smad1 and pSmad1 were distributed throughout mesangial cells with a preferential cytoplasmic localization after a 72 h-incubation in the presence of AGEs. Furthermore, the nuclear accumulation of Smad1 and pSmad1 in response to AGEs was observed in the cells 120 h after AGE stimulation, whereas BSA treatment led to little expression of Smad1 and pSmad1. The cells were counterstained with DAPI, and the nuclei were identified (data not shown). Similarly, both the Smad1 and pSmad1 proteins were detected in extracts from AGE-treated, but not BSA-treated, cells (Fig. 3*c*). These findings indicate that the regulation of Col4 is correlated with the expression of Smad1 under AGE exposure.

The Blocking of Smad1 Attenuates ECM Protein Overproduction—To examine the importance of the Smad1 signaling pathway for the AGE-induced overexpression of Col4, we selectively inhibited this pathway by the antisense (AS) gene. The AGE-

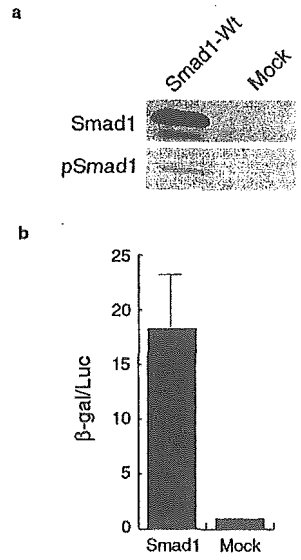

FIG. 2. **Effects of Smad1 on Col4 transcriptional activity.** *a*, cells were cotransfected with CIV-1-lacZ reporter plasmid and with either the vector encoding wild-type Smad1 (*Smad1-Wt*) or the vector alone (*Mock*), along with CMV-LUC as an internal control. Whole cell lysates were analyzed by Western blot with the anti-Smad1 and anti-pSmad1 antibody. One of three independent experiments is shown. *b*, after 48 h, cells were lysed, and β-galactosidase (*β-gal*) and luciferase (*Luc*) activities were measured. Values are the averages of triplicate determinations ±S.D.

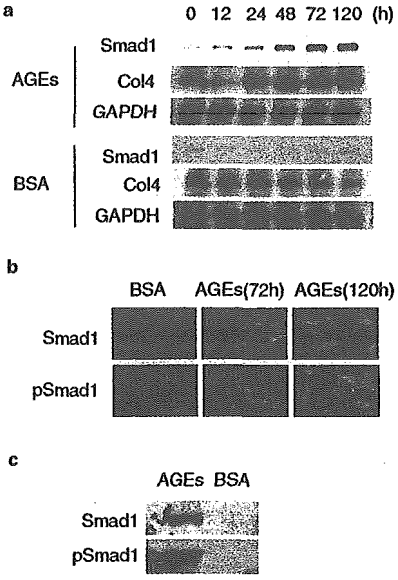

FIG. 3. **Exposure to AGEs causes dynamic changes in Smad1 expression.** *a*, RNase protection assay analysis of *Smad1* and *Col4* mRNA expression in total RNA lysates from mesangial cells treated with AGEs or BSA for the indicated time periods. Chronic stimulation of AGEs promotes *Smad1* continuous expression, paralleled with expression of *Col4*. One of three independent experiments is shown. Glyceraldehyde-3-phosphate dehydrogenase (*GAPDH*) was used as an internal control. *b*, immunofluorescence of mesangial cells after 72 or 120 h of treatment with AGEs or BSA. Data from one of three representative experiments is shown. *c*, Smad1 and pSmad1 were monitored by Western blot in response to a 72-h treatment with AGEs or BSA. One of three independent experiments is shown.

mediated induction of Smad1 was completely abolished in the presence of AS, but not in the presence of control oligos (4-mismatch) (Fig. 4, *a* and *b*). The overexpression of Col4 was strongly attenuated, consistent with the inhibition of Smad1. Similarly, both *Col1* and *OPN* mRNA levels were significantly

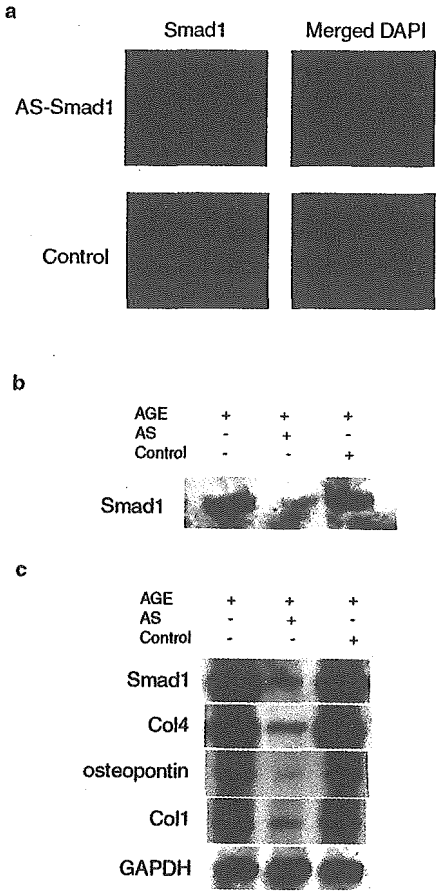

FIG. 4. **Effects of antisense oligo specific for Smad1 in mesangial cells.** *a*, immunofluorescence analysis of the antisense-treated mesangial cells, using the anti-Smad1 antibody (*green*) merged with DNA stained by DAPI (*blue*). After 72 h of incubation with AGEs, mesangial cells were incubated for 16 h in medium containing AS-Smad1 or 4-mismatch (*Control*). Data from one of three representative experiments is shown. *b*, Western blot analysis of Smad1 protein expression in mesangial cells treated with AGEs after transfection of AS or control. One of three independent experiments is shown. *c*, AS-Smad1 blocks the up-regulated mRNA levels of *Col4*, *osteopontin*, and *Col1* induced by AGEs treatment on mesangial cells. One of three independent experiments is shown.

decreased (Fig. 4*c*). Smad1 mismatch morpholino oligos (control) had no effect on the expression of these genes. These data indicate that Smad1 plays a critical role in the control of Col4 expression.

Smad1 and ALK1 Expression in Diabetic Conditions—To further elucidate the mechanism of Smad1 expression after AGE treatment, we investigated the expression of ALK1 in mesangial cells. ALK1 is a type I receptor for TGF-β family proteins and, specifically, phosphorylates Smad1 and Smad5. We were able to detect the significant increase in ALK1 mRNA expression in AGE-treated mesangial cells using an RNase protection assay (Fig. 5). In addition, at 10 μg/ml the TGF-β-neutralizing antibody significantly attenuated the up-regulated mRNA levels of *ALK1* and *Smad1* under AGE stimulation (data not shown). Furthermore, we examined whether high glucose exposure affected the expression of *ALK1*, *Smad1*, or *Col4*. In this condition, mRNA levels of these genes were increased, but they were weak and transient, compared with AGEs exposure (data not shown).

Finally, we investigated the glomerular expression of Smad1 and ALK1 in human diabetic nephropathy. We carried out indirect immunohistochemistry on renal biopsies (diabetic nephropathy) and on normal kidney tissue. Glomerular immunoreactivity for Smad1 and ALK1 was correlated with the severity of sclerotic lesions in diabetic renal glomeruli; the immunoreactive signal was nearly absent in normal glomeruli (Fig. 6). These histological observations suggest that the ALK1/Smad1 signaling pathway is linked to the ECM expansion.

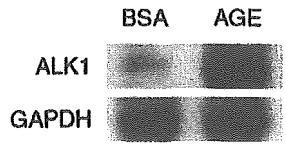

FIG. 5. **Regulation of ALK1 mRNA expression by AGEs.** After treatment with AGEs, the specific mRNAs were determined by using the RNase protection assay. The amount of total RNA loaded (1 μg/lane) was checked by hybridization with a glyceraldehyde-3-phosphate dehydrogenase (*GAPDH*) probe. The data are representative of three independent experiments.

DISCUSSION

Changes in GBM structure occur very earlier in diabetic nephropathy, even before microalbuminuria is apparent. Although Col4 is the principal component of the GBM, the cellular and molecular mechanisms involved in the up-regulation of Col4 in diabetic conditions are, as yet, poorly understood. We have reported previously that an unknown protein binds to the Col4 promoter under AGE exposure (9). Here, we identified the protein as Smad1 using a yeast one-hybrid system. It is generally acknowledged that Smad1 transduces BMP signals, inducing formation of bone and cartilage (22). Moreover, signaling by Smad1 is modulated by various other proteins such as signal transducers and activators of transcription 3 (STAT3) (27) and Smurf1 (28), allowing the TGF-β superfamily ligands to elicit diverse effects on target cells. Recently, mesangial cells have been shown to produce TGF-β when exposed to AGEs (29). We observed that chronic exposure of AGEs, inducing the sustained increase in *Smad1* gene activation and expression, leads to Col4 overproduction, suggesting that Smad1 is a critical modulator in diabetic conditions.

Targeted gene disruption of the *Smad1* gene in mice results in embryonic lethality, suggesting that Smad1 plays critical roles in early embryogenesis (30). However, because of the early embryonic lethality, not much is known about the role of Smad1 *in vivo*, particularly in the adult. A recent study has shown that Smad1 is absent in renal glomeruli in normal adult mouse (24). We show for the first time that AGEs induce the expression of Smad1 in adult mouse glomeruli. Therefore, Smad1 may be the earliest indicator of renal dysfunction.

Development of diabetic kidney disease in diabetic patients is a huge clinical problem associated with increased morbidity and mortality. It is also clear that the current therapy, optimal glycemic control, can slow (1, 2) but not prevent the development or progression of diabetic nephropathy in most patients. Previous studies have shown that TGF-β is a key mediator of ECM accumulation in experimental and human kidney disease, leading to progressive glomerular scarring and renal failure (10, 11). Therapeutic approaches to down-regulate TGF-β signaling under diabetic conditions provide one strategy for inhibiting the progression of diabetic nephropathy. For example, the use of the endogenous proteoglycan decorin (natural inhibitor of TGF-β) (31) and the use of a neutralizing TGF-β antibody (32) have been shown to prevent the development of diabetic glomerulosclerosis. However, prolonged inhibition of TGF-β may lead to unwanted adverse effects, because TGF-β has anti-proliferative effect in some cancers and, in one report, Smad3-deficient animals found metastatic colon tumors (33). Therefore, inhibitors for specific responses of TGF-β will lead to

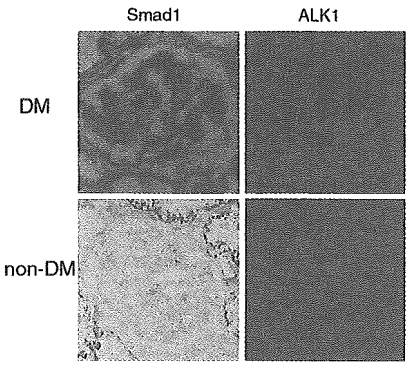

FIG. 6. **Detection of Smad1 and ALK1 in human diabetic kidney.** Immunohistochemical staining of glomeruli from kidneys of diabetic (*DM*; $n = 5$) or non-diabetic (*non-DM*; $n = 3$) patients stained with anti-Smad1 and anti-ALK1 antibodies. Glomerular positivity of Smad1 and ALK1 was prominently detectable in diabetic patients but not detectable in non-diabetic patients. All sections were counterstained with hematoxylin. Original magnification for all was ×400.

a novel therapeutic approach. We have demonstrated here that the morpholic antisense oligo specific for Smad1 strongly attenuated the overproduction of Col4 induced by AGEs. Similarly, Col1 and OPN mRNA expressions were partially inhibited. It is reported that Smad1 dissociates the repressor Hoxc-8 from the *OPN* promoter, thereby inducing *OPN* transcription (34). Thus, Smad1 may be a novel therapeutic target in diabetic complications and be useful in combination with the current therapy.

TGF-β evokes its biological effects by signaling through two different types of serine/threonine kinase receptors. Type II receptor activates type I receptors, which transduce various signals via the Smads (22, 26). Recent reports demonstrated that ALK1 has been thought of as a BMP signal transducer, mediating signals from TGF-β via Smad1 (13, 14). Therefore, we investigated the expression of ALK1 in mouse mesangial cells and human kidney tissues. We have also shown that ALK1 and Smad1 are expressed in renal glomeruli, corresponding to the progression of diabetic conditions. These results lead not only to a better understanding of the mechanisms responsible for the initiation and progression of diabetic conditions but also to the development of novel therapeutic strategies for the treatment of diabetic complications in various organs by suppressing the pathologically activated production of collagen. Both Smad1 and ALK1 are nearly absent in normal mesangial cells. In this study, we first demonstrated that ALK1 as well as Smad1 participate in the development of diabetic change in kidney, suggesting that ALK1 acts upstream of the excessive production of Col4.

AGEs are known to induce a variety of cellular events in vascular cells and other cells, possibly through the functional several AGEs receptors, thereby modulating the disease processes. AGEs have been recently accepted as having an important role, not only in diabetic complications but also in aging and old age-related diseases, including atherosclerosis (6, 7). Col4 is also a major component of the vascular basement membrane that lies beneath the endothelium, surrounds medial smooth muscle cells, and undergoes significant nonenzymatic glycosylation (glycation). Glycation leads ultimately to increased cross-linking of collagen, resulting in increased arterial stiffness (35). We report here that AGE-induced Col4 overproduction is mediated by Smad1 signaling. Recent reports show that Smad1 is expressed in endothelial cells of some blood vessels and is at the site of vasculogenesis in the developing yolk sac during blood island formation (36). Furthermore, ALK1 is highly expressed in vascular endothelial cells (22, 37) and may be essential for vascular maturation and stabilization (38, 39). Inactivating mutations of ALK1 result in human hereditary hemorrhagic telangiectasia 2, also known as Osler-Rendu-Weber syndrome (40). In addition, recent evidence indicates that Smad1 transcriptionally regulates the osteopontin gene (33), which is a key factor of the progression of renal injuries and atherosclerosis. Accordingly, we speculate that the ALK1/Smad1 signaling may mediate the development of atherosclerosis, both in diabetic patients and in the aged, by inducing an overproduction of ECM. Because diabetic renal disease in the human is a process that occurs slowly over many years, it is likely that a very detailed evaluation of this phenomenon will be required to determine the interaction of Smad1 and ALK1 in this condition. Further work is in progress to clarify the role of ALK1/Smad1 in diabetic kidney using animal models.

Acknowledgments—We thank Dr. K. Miyazono (The University of Tokyo, Japan) for providing a plasmid encoding Smad1 and Dr. Y. Takishita (Tokushima Prefectural Central Hospital, Japan) for his assistance with histological analysis. We also thank the members of our laboratory for discussions.

REFERENCES

1. The Diabetes Control and Complications Trial Research Group (1993) *N. Engl. J. Med.* **329,** 977–986
2. United Kingdom Prospective Diabetes Study (UKPDS) Group (1998) *Lancet* **352,** 837–853
3. Vlassara, H., Striker, L. J., Teichberg, S., Fuh, H., Li, Y. M., and Steffes, M. (1994) *Proc. Natl. Acad. Sci. U. S. A.* **91,** 11704–11708
4. Brownlee, M., Cerami, A., and Vlassara, H. (1988) *N. Engl. J. Med.* **318,** 1315–1321
5. Doi, T., Vlassara, H., Kirstein, M., Yamada, Y., Striker, G. E., and Striker, L. J. (1992) *Proc. Natl. Acad. Sci. U. S. A.* **89,** 2873–2877
6. Vlassara, H., Fuh, H., Makita, Z., Krungkrai, S., Cerami, A., and Bucala, R. (1992) *Proc. Natl. Acad. Sci. U. S. A.* **89,** 12043–12047
7. Huijberts, M. S., Wolffenbuttel, B. H., Boudier, H. A., Crijns, F. R., Kruseman, A. C., Poitevin, P., and Levy, B. I. (1993) *J. Clin. Investig.* **92,** 1407–1411
8. Park, L., Raman, K. G., Lee, K. J., Lu, Y., Ferran, L. J., Jr., Chow, W. S., Stern, D., and Schmidt, A. M. (1998) *Nat. Med.* **9,** 1025–1031
9. Iehara, N., Takeoka, H., Yamada, Y., Kita, T., and Doi, T. (1996) *Kidney Int.* **50,** 1166–1172
10. Yang, C. W., Vlassara, H., Peten, E. P., He, C. J., Striker, G. E., and Striker, L. J. (1994) *Proc. Natl. Acad. Sci. U. S. A.* **91,** 9436–9440
11. Sanderson, N., Factor, V., Nagy, P., Kopp, J., Kondaiah, P., Wakefield, L., Roberts, A. B., Sporn, M. B., and Thorgeirsson, S. S. (1995) *Proc. Natl. Acad. Sci. U. S. A.* **92,** 2572–2576
12. ten Dijke, P., Miyazono, K., and Heldin, C. H. (1996) *Curr. Opin. Cell Biol.* **8,** 139–145
13. Oh, S. P., Seki, T., Goss, K. A., Imamura, T., Yi, Y., Donahoe, P. K., Li, L., Miyazono, K., ten Dijke, P., Kim, S., and Li, E. (2000) *Proc. Natl. Acad. Sci. U. S. A.* **97,** 2626–2631
14. Chen, Y. G., and Massague, J. (1999) *J. Biol. Chem.* **274,** 3672–3677
15. Floege, J., Johnson, R. J., Gordon, K., Iida, H., Pritzl, P., Yoshimura, A., Campbell, C., Alpers, C. E., and Couser, W. G. (1991) *Kidney Int.* **40,** 477–488
16. Bruggeman, L. A., Burbelo, P. D., Yamada, Y., and Klotman, P. E. (1992) *Oncogene* **7,** 1497–1502
17. Davies, M. (1994) *Kidney Int.* **45,** 320–327
18. Burbelo, P. D., Utani, A., Pan, Z. Q., and Yamada, Y. (1993) *Proc. Natl. Acad. Sci. U. S. A.* **90,** 11543–11547
19. Luo, R. X., Postigo, A. A., and Dean, D. C. (1998) *Cell* **92,** 463–473
20. Abe, H., Iehara, N., Utsunomiya, K., Kita, T., and Doi, T. (1999) *J. Biol. Chem.* **274,** 20874–20878
21. Ahn, D. G., Kourakis, M. J., Rohde, L. A., Silver, L. M., and Ho, R. K. (2002) *Nature* **417,** 754–758
22. Massague, J., and Wotton, D. (2000) *EMBO J.* **19,** 1745–1754
23. Roelen, B. A., van Rooijen, M. A., and Mummery, C. L. (1997) *Dev. Dyn.* **209,** 418–430
24. Huang, S., Flanders, K. C., and Roberts, A. B. (2000) *Gene* **258,** 43–53
25. Kusanagi, K., Inoue, H., Ishidou, Y., Mishima, H. K., Kawabata, M., and Miyazono, K. (2000) *Mol. Biol. Cell* **11,** 555–565
26. Heldin, C. H., Miyazono, K., and ten Dijke, P. (1997) *Nature* **390,** 465–471
27. Nakashima, K., Yanagisawa, M., Arakawa, H., Kimura, N., Hisatsune, T., Kawabata, M., Miyazono, K., and Taga, T. (1999) *Science* **284,** 479–482
28. Zhu, H., Kavsak, P., Abdollah, S., Wrana, J. L., and Thomsen, G. H. (1999) *Nature* **400,** 687–693
29. Throckmorton, D. C., Brogden, A. P., Min, B., Rasmussen, H., and Kashgarian, M. (1995) *Kidney Int.* **48,** 111–117
30. Tremblay, K. D., Dunn, N. R., and Robertson, E. J. (2001) *Development* **128,** 3609–3621
31. Isaka, Y., Brees, D. K., Ikegaya, K., Kaneda, Y., Imai, E., Noble, N. A., and Border, W. A. (1996) *Nat. Med.* **2,** 418–423
32. Chen, S., Carmen, Iglesias-de la Cruz, M., Jim, B., Hong, S. W., Isono, M., and

Ziyadeh, F. N. (2003) *Biochem. Biophys. Res. Commun.* **300,** 16–22
33. Zhu, Y., Richardson, J. A., Parada, L. F., and Graff, J. M. (1998) *Cell* **94,** 703–714
34. Shi, X., Yang, X., Chen, D., Chang, Z., and Cao, X. (1999) *J. Biol. Chem.* **274,** 13711–13717
35. Chappey, O., Dosquet, C., Wautier, M. P., and Wautier, J. L. (1997) *Eur. J. Clin. Investig.* **27,** 97–108
36. Dick, A., Risau, W., and Drexler, H. (1998) *Dev. Dyn.* **211,** 293–305
37. Attisano, L., Carcamo, J., Ventura, F., Weis, F. M., Massague, J., and Wrana, J. L. (1993) *Cell* **75,** 671–680
38. Urness, L. D., Sorensen, L. K., and Li, D. Y. (2000) *Nat. Genet.* **26,** 328–331
39. Larsson, J., Goumans, M. J., Sjostrand, L. J., van Rooijen, M. A., Ward, D., Leveen, P., Xu, X., ten Dijke, P., Mummery, C. L., and Karlsson, S. (2001) *EMBO J.* **20,** 1663–1673
40. Johnson, D. W., Berg, J. N., Baldwin, M. A., Gallione, C. J., Marondel, I., Yoon, S. J., Stenzel, T. T., Speer, M., Pericak-Vance, M. A., Diamond, A., Guttmacher, A. E., Jackson, C. E., Attisano, L., Kucherlapati, R., Porteous, M. E., and Marchuk, D. A. (1996) *Nat. Genet.* **13,** 189–195

THE JOURNAL OF BIOLOGICAL CHEMISTRY
Vol. 279, No. 19, Issue of May 7, pp. 19816–19823, 2004
Printed in U.S.A.

Advanced Glycation End Products Increase Collagen-specific Chaperone Protein in Mouse Diabetic Nephropathy*

Received for publication, September 22, 2003, and in revised form, February 24, 2004
Published, JBC Papers in Press, March 5, 2004, DOI 10.1074/jbc.M310428200

Seiji Ohashi‡, Hideharu Abe‡, Toshikazu Takahashi‡, Yasuhiko Yamamoto§, Masayoshi Takeuchi¶, Hidenori Arai‖, Kazuhiro Nagata, Toru Kita‡‡, Hiroshi Okamoto§§, Hiroshi Yamamoto§, and Toshio Doi‡¶¶**

*From the ‡Department of Clinical Biology and Medicine, Course of Biological Medicine, School of Medicine, The University of Tokushima, Tokushima 770-8503, Japan, §Department of Biochemistry and Molecular Vascular Biology, Kanazawa University Graduate School of Medical Science, Kanazawa 920-8640, Japan, ¶Department of Biochemistry, Faculty of Pharmaceutical Science, Hokuriku University, Kanazawa 920-1181, Japan, ‖Department of Geriatric Medicine, **Department of Molecular and Cellular Biology, Institute for Frontier Medical Sciences, ‡‡Department of Cardiovascular Medicine, Kyoto University, Kyoto 606-8575, Japan, and §§Department of Biochemistry, Tohoku University Graduate School of Medicine, Sendai 980-8575, Japan*

Advanced glycation end products (AGEs) appear to contribute to the diabetic complications. This study reports the inhibitory effect of OPB-9195 (OPB), an inhibitor of AGEs formation, and the role of a collagen-specific molecular chaperone, a 47-kDa heat shock protein (HSP47) in diabetic nephropathy. Transgenic mice carrying nitric-oxide synthase cDNA fused with insulin promoter (iNOSTg) leads to diabetes mellitus. The iNOSTg mice at 6 months of age represented diffuse glomerulosclerosis, and the expression of HSP47 was markedly increased in the mesangial area in parallel with increased expression of types I and IV collagens. OPB treatment ameliorated glomerulosclerosis in the iNOSTg mice associated with the decreased expression of HSP47 and types I and IV collagens. The expression of transforming growth factor-β (TGF-β) was increased in glomeruli of iNOSTg mice and decreased after treatment with OPB. To confirm these mechanisms, cultured mesangial cells were stimulated with AGEs. AGEs significantly increased the expression of HSP47, type IV collagen, and TGF-β mRNA. Neutralizing antibody for TGF-β inhibited the overexpression of both HSP47 and type IV collagen *in vitro*. In conclusion, AGEs increase the expression of HSP47 in association with collagens, both *in vivo* and *in vitro*. The processes may be mediated by TGF-β.

Nephropathy is a morbid complication associated with diabetes mellitus and is the leading cause of end-stage renal disease (1). Diabetic nephropathy is characterized by a mesangial expansion followed by glomerulosclerosis. The mechanism of these processes remains unknown. Advanced glycation end products (AGEs)[1] have been recently reported to play an important role in the pathogenesis of diabetic complications, particularly in the progression of retinopathy and nephropathy (2). AGEs, late compounds formed from early Amadori compounds produced during the Maillard reaction, slowly accumulate in various tissues. Direct evidence indicating the importance of AGEs in the progression of diabetic nephropathy has been reported previously (3–5). The administration of exogenous AGEs to normal rats induces glomerular hypertrophy and mesangial sclerosis, gene expression of matrix proteins, and production of various growth factors. An inhibitor of AGEs formation, aminoguanidine, ameliorates the mild glomerular changes and functional changes found in streptozocin-induced diabetic rats (6). Recently, a synthetic thiazolidine derivative, OPB-9195, was shown to have a strong inhibitory effect of AGE formation (7).

The 47-kDa heat shock protein (HSP47) has been identified as a collagen-binding stress protein and plays a role in the intracellular processing of procollagen molecules as a collagen-specific molecular chaperone. We recently reported that the expression of HSP47 was markedly increased in parallel with the development of glomerulosclerosis in a rat renal ablation model (8). We also found that the inhibition of HSP47 ameliorated glomerulosclerosis (9). Despite a possible pathophysiological role of collagen-binding HSP47 in the fibrotic process in various organs, factors that modulate its expression remain undefined.

To understand the pathogenesis of diabetic nephropathy and to develop prophylactic and therapeutic measures against it, suitable animal models are needed. However, no single animal model that develops the renal changes seen in humans is available. Spontaneously diabetic animals such as the non-obese diabetic mouse develop only limited lesions, at most mild mesangial sclerosis (10). The same is the case with chemically induced diabetic rodents. In this study, we analyzed transgenic mice carrying the mouse, type 2-inducible nitric-oxide synthase (iNOS) cDNA under the control of an insulin promoter (iNOSTg) (11). The nitric oxide-mediated destruction of β cells results in a markedly reduced pancreatic islet mass and in the development of type 1 diabetes mellitus. These characteristics were followed by glomerulosclerosis that resembled human diabetic nephropathy (3).

Transforming growth factor (TGF)-β was originally identified in neoplastic cells and subsequently reported to be present

* This work was supported in part by the "Research for the Future" Program for the Promotion of Science (Grant 97L00805). The costs of publication of this article were defrayed in part by the payment of page charges. This article must therefore be hereby marked "*advertisement*" in accordance with 18 U.S.C. Section 1734 solely to indicate this fact.

¶¶ To whom correspondence should be addressed: Dept. of Clinical Biology and Medicine, Course of Biological Medicine, School of Medicine, The University of Tokushima, 3-18-15 Kuramoto-cho, Tokushima 770-8503, Japan. Tel.: 81-88-633-7184; Fax: 81-88-633-9245; E-mail: doi@clin.med.tokushima-u.ac.jp.

[1] The abbreviations used are: AGEs, advanced glycation end-products; HSP47, 47-kDa heat shock protein; iNOS, inducible nitric-oxide synthase; OPB, OPB-9195; TGF, transforming growth factor; CML, carboxymethyllysine; BSA, bovine serum albumin; GAPDH, glyceraldehyde-3-phosphate dehydrogenase; siRNA, small interfering RNA.

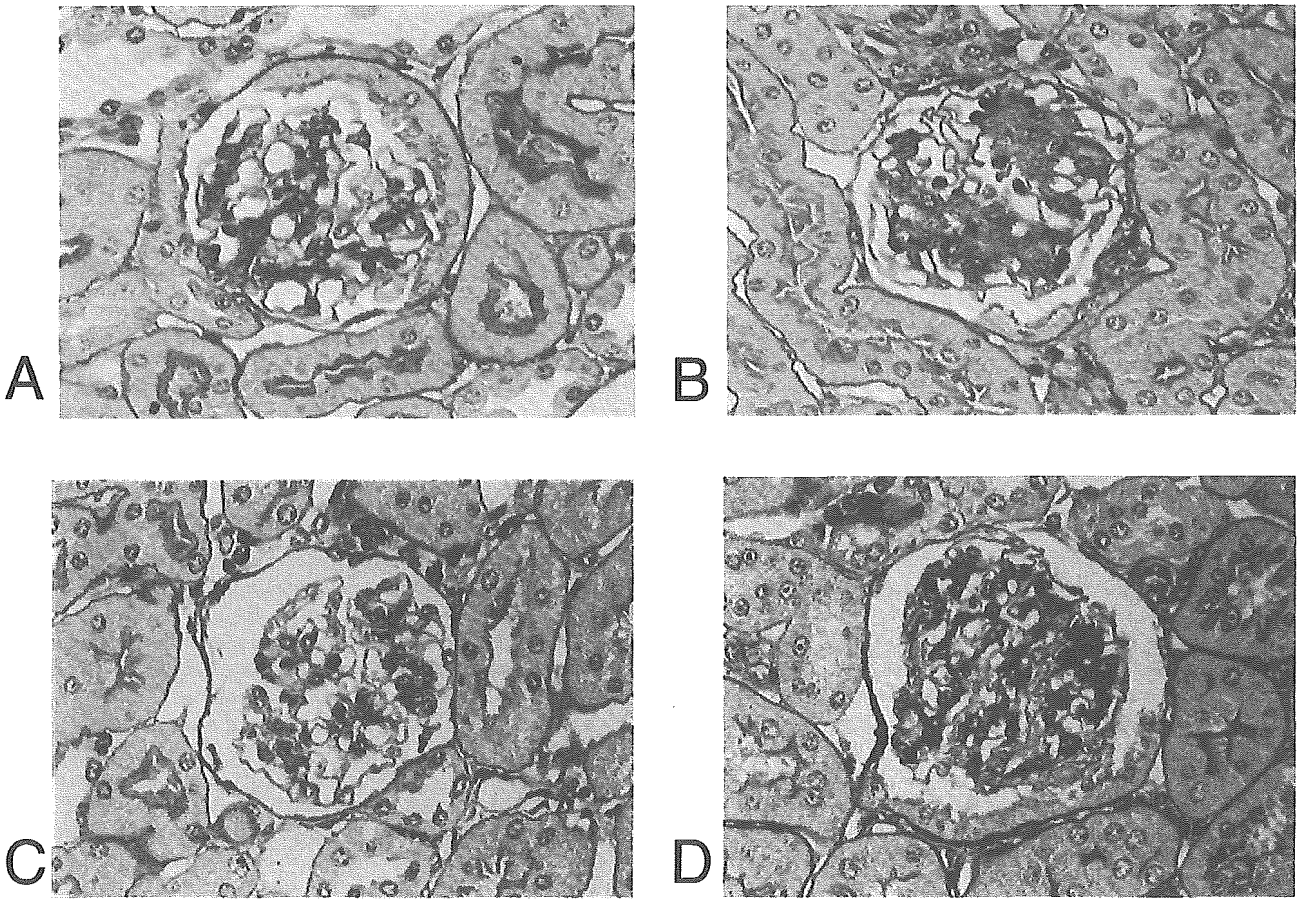

FIG. 1. **Light microscopy examination.** The microscopic lesions in iNOSTg mice took the form of diffuse proliferation of mesangial matrix and an expansion of the mesangial area. These lesions were ameliorated by treatment with OPB. *A*, control. *B*, iNOSTg. *C*, control + OPB. *D*, iNOSTg + OPB.

in most cells in which it exerts a variety of effects on cell proliferation, cell differentiation, and embryogenesis. It has also been shown to stimulate the production of extracellular matrix components including collagens and fibronectin and to play a pivotal role in fibrogenesis (12). Thus, TGF-β is considered to be a mediator of collagen production in the models of fibrogenesis. Significant progress has recently been made in our understanding of the expression of the collagen genes and their transcriptional regulation by TGF-β (8, 9). A recent report has shown that high glucose transiently induces a transcriptional activity of c-*fos* responsible for stimulation of the TGF-β (13). However, there is little information regarding the interaction between AGE and c-*Fos*. We investigated here the expression of c-*Fos* in cultured mesangial cells treated with AGE and examined whether c-*Fos* affected the expression of TGF-β.

Furthermore, our recent report demonstrates that type IV collagen is up-regulated by AGE and its overexpression is transcriptionally regulated by Smad1 (14). Smad1 also enhances the levels of expression of type I collagen and osteopontin and plays a critical role in TGF-β-mediated overexpression of extracellular matrix in diabetic nephropathy (14). Therefore, we examined the role of Smad1 for regulating HSP47 expression by AGE stimulation in mesangial cells.

In this study, we reported on a study of the inhibitory effect of OPB-9195 (OPB), a novel inhibitor of AGEs formation, in a model of diabetic nephropathy. The pathogenic role of HSP47 in the development of the glomerulosclerotic lesions in diabetes was examined. We also confirmed the mechanism of these processes with the use of cultured mesangial cells.

MATERIALS AND METHODS

Experimental Animals—iNOSTg were maintained on CD-1 mouse background (11). Male littermates were screened for the transgenes by the PCR amplification and used for analysis. The primers used for the detection of iNOSTg were as follows: forward primer, 5′-GTGGGCTATGGGTTTGTGGAAGGAGA-3′, and reverse primer 5′-CGATGTCACATGCAGCTTGT-3′.

No expression of iNOS protein, whose synthesis is directed only in pancreatic islets, was detected in the kidney. The mice were divided into four groups: CD-1 as control mice (Control); control mice treated with OPB (Control + OPB); iNOSTg; and iNOSTg treated with OPB (iNOSTg + OPB). Each group was fed either normal chow or the chow containing 0.28% OPB (provided by Fujii Memorial Research Institute, Otsuka Pharmaceutical, Tokushima, Japan) from 1 to 6 months after birth.

Blood Glucose and HbA1c Concentration—The levels of blood glucose and HbA1c were measured from the tail vein blood using Dexter Z sensor (Bayer-Medical, Tokyo, Japan) and DCA2000 analyzer (Bayer-Medical), respectively.

Determination of AGEs Concentration—Levels of serum carboxymethyllysine (CML) and non-CML AGEs were determined using a competitive enzyme-linked immunosorbent assay as described previously (15). 1 unit/ml CML or non-CML AGEs corresponded to a protein concentration of 1 μg/ml CML-bovine serum albumin (BSA) or non-CML AGE-BSA, respectively.

Renal Histology and Morphometric Analysis—Kidneys were processed for light microscopy examination, and the severity of the renal sclerosis was scored on an arbitrary scale from 0 to 4. The mean glomerular volume was determined as described previously (3, 16).

Immunofluorescence Analysis for HSP47, Types I and IV Collagens, and TGF-β—Immunofluorescence analysis was carried out as described previously using an affinity-purified polyclonal antibody specific to HSP47, types I and IV collagens, and TGF-β (8, 9).

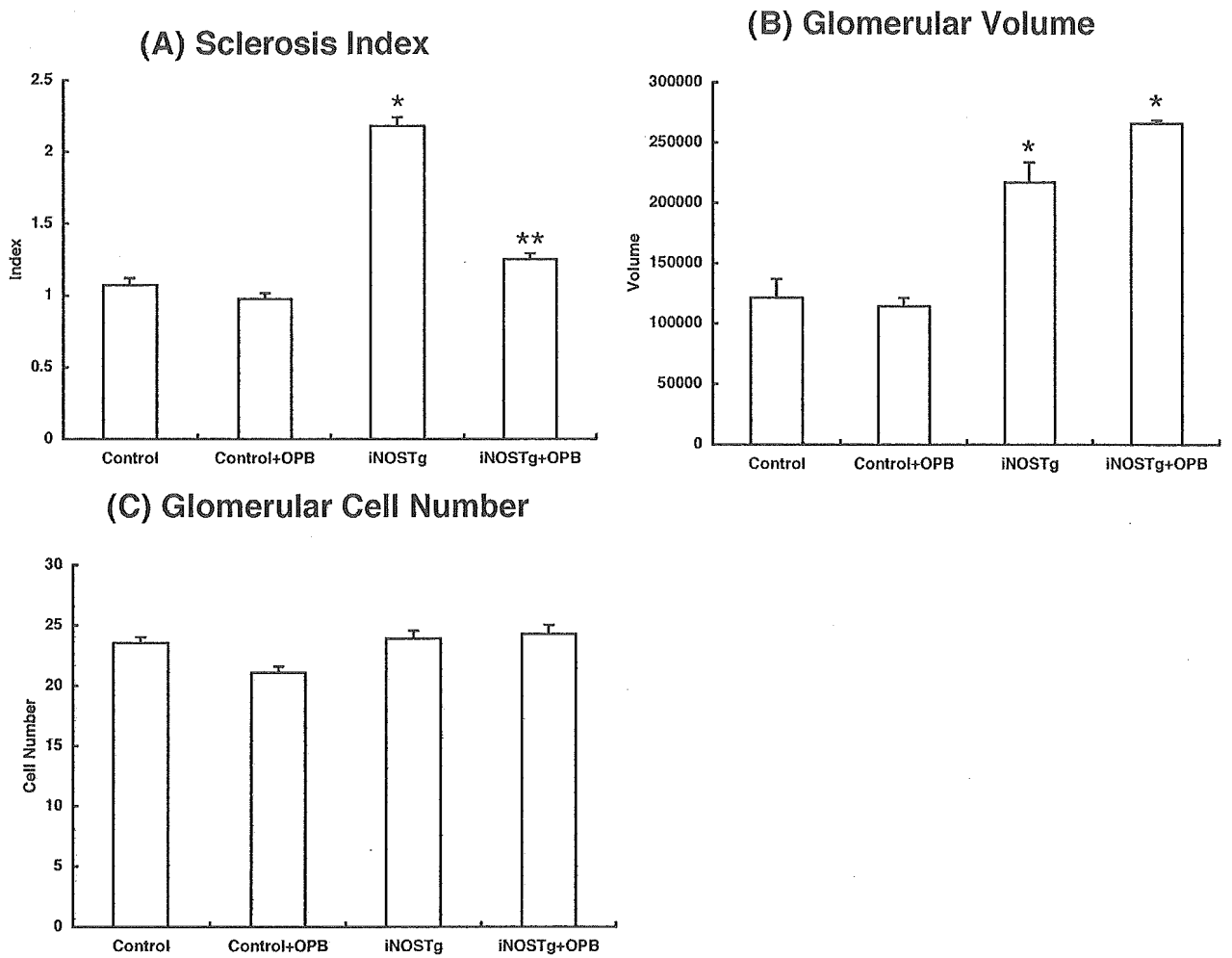

FIG. 2. **Effects of OPB in diabetic glomerulosclerosis.** OPB markedly improved glomerulosclerosis in iNOSTg mice (*A*) with no decrease in of glomerular volume (*B*). *C*, no significant differences in glomerular cell number were found. Number of experiments: Control, 11; OPB(−), 9; and OPB(+), 10. *, $p < 0.05$ *versus* Control; **, $p < 0.05$, OPB(+) *versus* OPB(−).

Laser-manipulated Microdissection and Laser Pressure Catapulating—Laser-manipulated microdissection is a method to cut out a small region from a specimen under microscope observation by means of laser beam. Laser pressure catapulating is a method to push up and collect samples that have been microdissected using laser-manipulated microdissection by means of a strong laser. These methods were performed using the Robot-Microbeam (P.A.L.M) and an inverted microscope (Carl Zeiss, Oberkochem, Germany) (17). By tracing around the glomeruli shown on the monitor, the targeted glomeruli were cut out by the laser. For laser pressure catapulating, the setting for the laser energy should be sufficiently high to catapult the microdissected glomeruli of the histologic specimen into the microcentrifuge cap, which was held in place by the micromanipulator. When the laser pressure catapulating was performed, the microdissected glomeruli "jumped up" and were attached to the cap. 60–80 glomeruli for each experiment were collected from this procedure. Glomeruli were obtained from those of control, iNOSTg, and iNOSTg-OPB mice at 24 weeks of age.

Quantitative PCR—Total RNA was prepared from isolated glomeruli, and a cDNA synthesis was performed with reverse transcription. Real-time PCR was performed by using the ABI Prism 7700 sequence detection system (PerkinElmer Life Sciences). Primers for mouse glyceraldehyde-3-phosphate dehydrogenase (*GAPDH*) (PerkinElmer Life Sciences) were used for internal control. The primers for HSP47, type IV collagen, and TGF-β were as follows: HSP47 (forward primer, 5′-GCGAGATAATCAGAGCGGCT-3′; reverse primer, 5′-CCACGCCCACTCTTGGACT-3′; and *Taq*Man Probe, 5′-CTTGCTCTTCATTGGCCGCCTGG-3′); type IV collagen (forward primer, 5′-GACCCCGAGGTTAGGAAGG-3′; reverse primer, 5′-CACTCGGTCCATGATCCCA-3′; and *Taq*Man Probe, 5′-ATCGAGCCGAGCCTAGAGCTGAAAGA-3′); and TGF-β (forward primer, 5′-AAGTCACCCGCGTGCTAATG-3′; reverse primer, 5′-CCCGAATGTCTGACGTATTGAA-3′; and *Taq*Man Probe, 5′-TGGACCGCAACAACGCAATCTATG-3′).

The cleavage of the sequence-specific probe (*Taq*Man Probe) by 5′-nuclease activity of the *Taq*DNA polymerase releases the reporter dye, resulting in an emission increase. With each cycle, the fluorescence intensity of additional reporter dye molecules is monitored by the system. The threshold cycles were selected in the line in which all of the samples were in the logarithmic phase. The quantity of PCR products was calculated from the threshold cycle value. This real-time detection generates quantitative data based on PCR at early cycles when PCR fidelity is highest (18, 19).

Cell Culture—A glomerular mesangial cell line was established from glomeruli isolated from normal 4-week-old mice (C57BL/6JxSJL/J) and was identified according to a method described previously (4, 5). The mesangial cells were plated on 100-mm plastic dishes (Nunc) that were maintained in B medium (a 3:1 mixture of minimal essential medium/F12 modified with trace elements) supplemented with 1 mM glutamine, penicillin at 100 units/ml, streptomycin at 100 μg/ml, and 20% fetal calf serum (Irvine Scientific). The cells were passaged weekly with trypsin-EDTA. The cultured cells fulfilled the previously described criteria generally accepted for glomerular mesangial cells (20).

AGE-BSA—AGE-BSA was prepared by the method described previously (5, 21). BSA was incubated with glucose 6-phosphate for >60 days at 37 °C. AGE content was measured by the fluorescence intensity at a protein concentration of 1 mg/ml. Control BSA was prepared by incubating BSA without glucose 6-phosphate under the same conditions as those for AGE-BSA. AGE-BSA and control BSA contained 61.3 and 8.31 AGE units/mg protein, respectively. Protein concentrations were determined by the method of Bradford using BSA as the standard.

Mesangial cells were plated in the B medium, 20% fetal bovine serum at 5×10^5/well in six-well dishes, that had been coated with AGE-BSA or control BSA at 50 μg/cm^2 for 72 h. After the treatment, the cells were

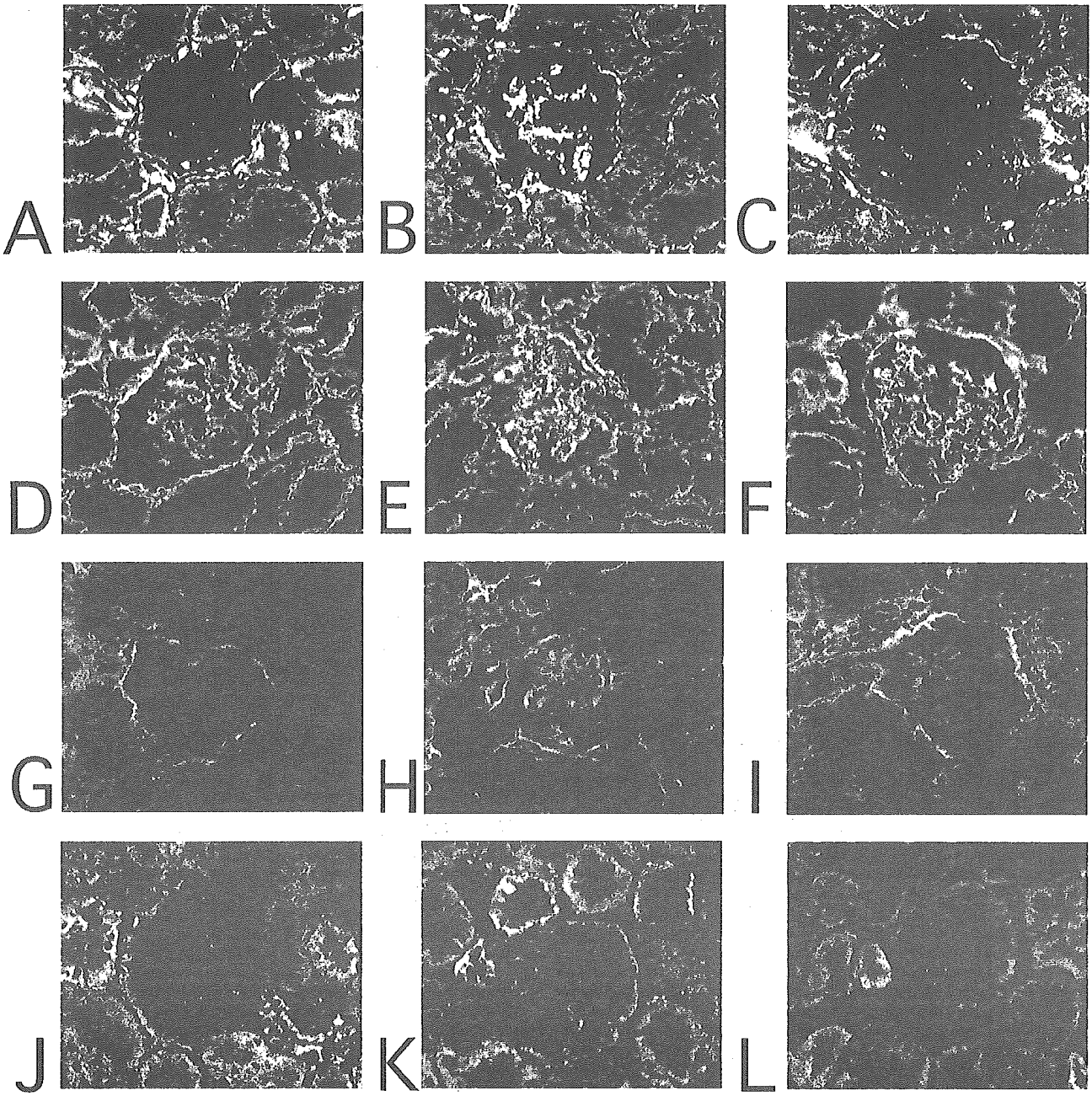

FIG. 3. **Immunofluorescence analysis of HSP47, collagens, and TGF-β.** A remarkable increase in the expression of HSP47, types I and IV collagens, and TGF-β was seen. OPB treatment led to show a significant decrease. *A–C*, type I collagen; *D–F*, type IV collagen. *G–I*, HSP47. *J–L*, TGF-β. *A*, *D*, *G*, and *J*, control. *B*, *E*, *H*, and *K*, iNOSTg. *C*, *F*, *I*, and *L*, iNOSTg + OPB.

washed with phosphate-buffered saline and total RNA was isolated using TRIzol reagent (Invitrogen).

TGF-β-neutralizing Antibody Assay—The cells were resuspended at a concentration of 1×10^6 cells/ml and plated onto 100-mm dish either in the presence of 10 μg/ml TGF-β1-neutralizing antibody (R&D Systems) or a control normal IgG (22). After 24 h of incubation, the cells were harvested and underwent RNA isolation on real-time reverse transcription-PCR.

Smad1 Morpholino Antisense Oligonucleotide—The antisense oligonucleotide for *Smad1* was a 25-nucleotide morpholino oligomer (Genetools LLC) with the base composition of 5′-CAAGCTGGTCACATTCATAGCGGCT-3′. A standard morpholino oligomer with the base composition of 5′-CAtGCTcGTCACATTCAaAGCcGCT-3′ (points of mismatch are shown by *small letters*) was used as a control. Microinjection of *in vitro* transcribed RNA was performed as described previously (14).

Western Blotting—Cultured mesangial cells were harvested in sample buffer, resolved by SDS-polyacrylamide gel electrophoresis, transferred to nitrocellulose membrane, subjected to Western blot using a 1:500 dilution of antibody for HSP47, type IV collagen, and TGF-β (8, 9), and detected using an enhanced chemiluminescence detection system (Invitrogen).

RNase Protection Assay—Total RNA was isolated from mesangial cells using the TRIzol reagent, and an RNase protection assay was performed as described previously (14, 22). The RNA probes were prepared by linearizing the PvuII fragment of type IV collagen from p1234, the SacI fragment of *Smad1* from pGEM-T, and the EcoRI fragment of *GAPDH* from pMGAP1. In addition, mouse riboprobe for HSP47 (5′-TCCTATACTGTGGGTGTTACGATGA-3′ and 5′-TACAACTCATCTCGCATCTTGTCTC-3′), c-*fos* (5′-TATCTCCTGAAGAGGAAGAGAAACG-3′ and 5′-AACAAGAAGTCATCAAAGGGTTCTG-3′), and TGF-β (5′-ATACCAACTATTGCTTCAGCTCCAC-3′ and 5′CACGTAGTAGACGATGGGCAGT-3′) was amplified by reverse transcription-PCR. The PCR fragments were sequenced to confirm to be cDNAs, respectively, and

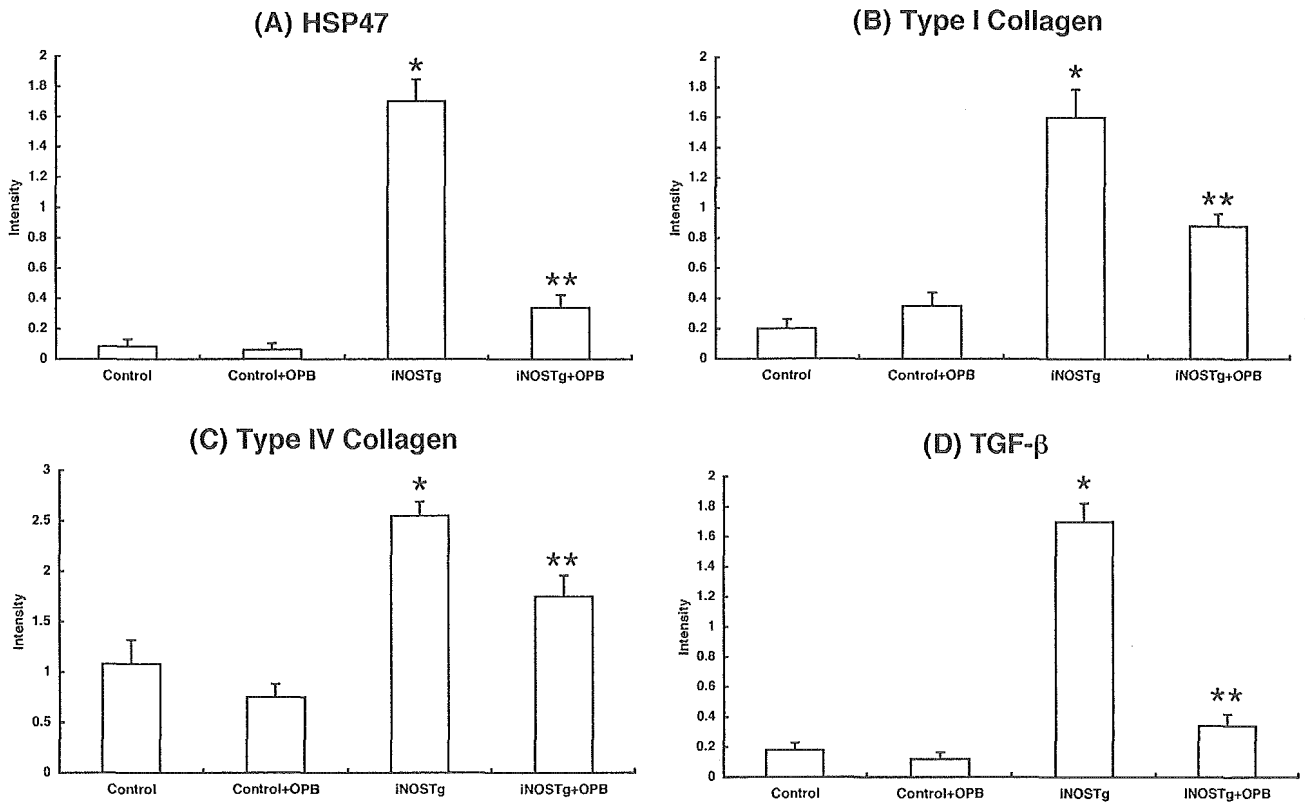

FIG. 4. **Arbitrary scaling of expressions of HSP47, collagens, and TGF-β.** A remarkable increase in the expression of HSP47 (*A*), types I (*B*) and IV (*C*) collagens, and TGF-β (*D*) was seen. OPB treatment showed a significant decrease. *, $p < 0.05$; *versus* Control; **, $p < 0.05$, OPB(+) *versus* OPB(−).

were cloned into a pGEM-T plasmid. After digesting the plasmid with SacI, an antisense riboprobe was synthesized *in vitro* using T7 RNA polymerase. The RNA probes and the test RNA were hybridized overnight at 45 °C. RNase A (40 μg/ml) and RNase T1 (2 μg/ml) were added to each tube, and the tubes were incubated for 1 h at 30 °C. The RNase resistant fragments were analyzed by 5% polyacrylamide, 8 M urea gel electrophoresis. The protected bands for each RNA probe had the same size as the coding sequence for the specific mRNA.

Small Interfering RNA (siRNA) and Transfections—The siRNA sequence targeting c-*fos* (5′-CCAATCTGCTGAAGAGAAGGAAAA-3′) was purchased from Hokkaido Science (Sapporo, Japan). Cells were transfected with LipofectAMINE 2000 (Invitrogen) according to the manufacturer's protocol in the presence of siRNA. siRNA against *Luciferase GL2* (5′-CGTACGCGGAATACTTCGA-3′) (Dharmacon) was used as a control.

RESULTS

Blood Glucose, HbA1c, and AGE Concentration—Blood glucose levels of iNOSTg mice were >500 mg/dl (503 ± 19 mg/dl, $n = 9$), and OPB had no effect on this parameter (586 ± 74 mg/dl, $n = 5$). HbA1c levels were over 7% in iNOSTg mice (7.5 ± 0.8%), whereas that of controls was below the detection limit. Both serum levels of CML and non-CML AGEs were significantly higher in iNOSTg mice (7.3 ± 0.6 and 20.7 ± 2.5 units/ml, respectively) than controls (6.2 ± 0.4 and 12.6 ± 1.0 units/ml, respectively), whereas OPB treatment of iNOSTg mice led to a decrease to the control levels (4.3 ± 1.0 and 10.2 ± 2.6 units/ml, respectively).

Response of Matrix Expansion to Treatment with OPB—The microscopic lesions in iNOSTg mice were observed as a diffuse proliferation of the mesangial matrix and the expansion of the mesangial area (Fig. 1). These lesions were ameliorated by treatment with OPB. OPB markedly improved the glomerulosclerosis of iNOSTg mice with no decrease in glomerular volume. No significant differences in glomerular cell number were detected among these groups (Fig. 2).

Response of Expressions of Collagens and HSP47 to Treatment with OPB—Although only traces of type I collagen could be detected in control glomeruli, it was strongly expressed in the mesangial area of glomeruli in iNOSTg mice. OPB treatment decreased this expression. Type IV collagen was expressed in both the glomerular basement membrane and the mesangium in control mice. Mesangial expression was increased in iNOSTg mice, which decreased after treatment with OPB. Immunofluorescent staining also revealed a remarkable increase in the expression of HSP47, which paralleled the expression of type I and type IV collagen and TGF-β in iNOSTg mice. These expressions were decreased as the result of OPB treatment (Figs. 3 and 4).

Quantitation of the Expression Ratio of HSP47/GAPDH mRNA and Type IV Collagen/GAPDH mRNA in Glomeruli by Real-time RT-PCR—Isolated mRNA of 50 glomeruli randomly selected from 5-μm frozen sections by laser-manipulated microdissection and laser pressure catapulating was used to quantitate the expression of HSP47 and type IV collagen mRNA in this diabetic nephropathy model. A remarkable increase in the expression of HSP47, type IV collagen, and TFG-β was seen in iNOSTg mice, and OPB treatment showed a significant decrease (Fig. 5).

Stimulation by AGEs in Cultured Mesangial Cells—To confirm the mechanism, cultured mesangial cells were stimulated with AGEs. AGEs significantly increased both HSP47 and type IV collagen expressions. In addition, AGEs were found to enhance the expression of TGF-β in cultured mesangial cells (Fig. 6*a*). Similarly, the levels of both HSP47 and type IV collagen proteins increased in accordance with the elevation of TGF-β protein (Fig. 6*b*). Neutralizing antibody for TGF-β inhibited overexpression of both HSP47 and type IV collagen (Fig. 7, *a* and *b*).

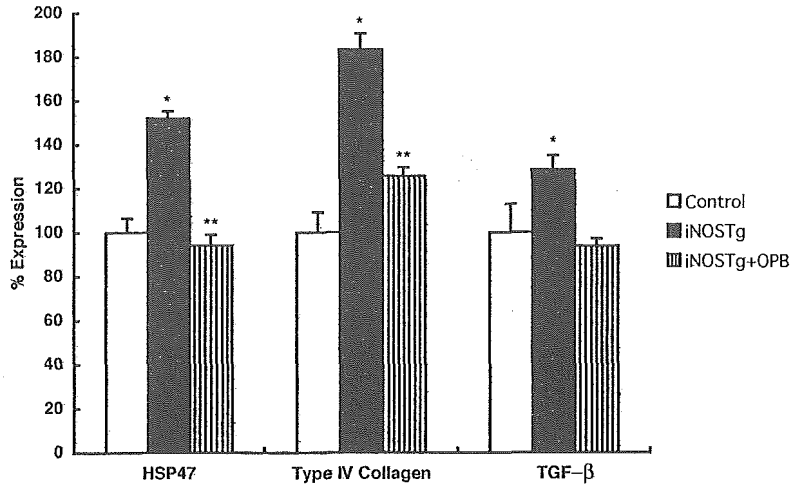

FIG. 5. **Glomerular mRNA expression.** Number of experiments: Control, 4; OPB(−), 5; and OPB(+), 6. *, $p < 0.05$ *versus* Control; **, $p < 0.05$, OPB(+) *versus* OPB(−).

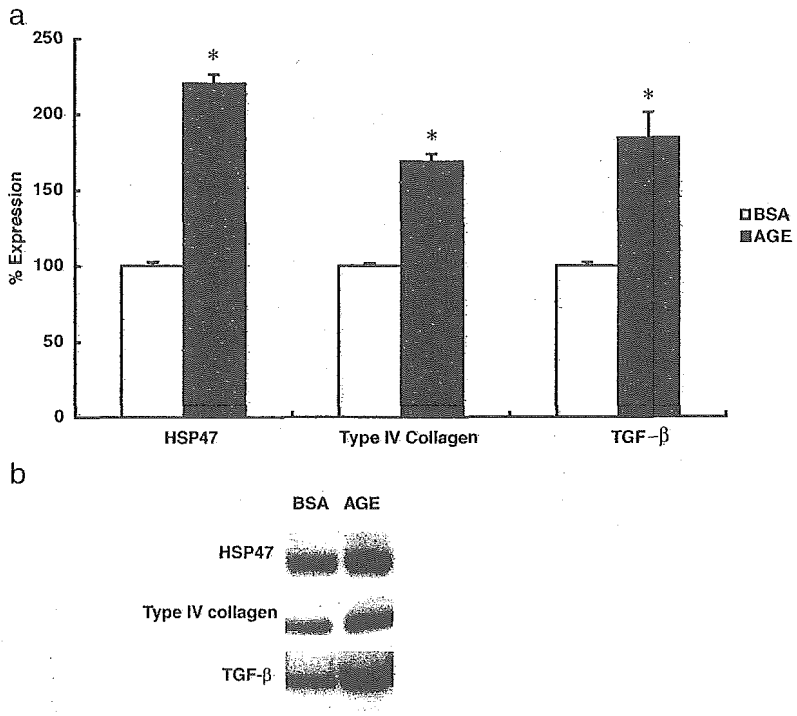

FIG. 6. **Effects of AGE in cultured mesangial cells.** *a*, AGE stimulation increased mRNA expressions of HSP47, TGF-β, and type IV collagen in cultured mesangial cells (number of experiments, 5). *, $p < 0.05$ *versus* Control (BSA). *b*, HSP47, type IV collagen, and TGF-β were monitored by Western blot in response to a 72-h treatment with AGE or BSA. One of three independent experiment is shown.

To further elucidate the mechanism for AGE-mediated induction of TGF-β, we investigated the expression of c-*fos* in mesangial cells. We found that AGE treatment caused a significant increase of c-*fos* mRNA by RNase protection assay. The AGE-mediated induction of c-*fos* was completely abolished in the presence of the specific siRNA but not in the presence of control siRNA. Consistent with the inhibition of c-*fos*, the induction of TGF-β was strongly attenuated (Fig. 8).

We next examined the involvement of Smad1 in TGF-β-mediated induction of HSP47 and type IV collagen expression. We transfected antisense morpholino oligomers to block Smad1-mediated effect in mesangial cells. Mesangial cells transfected with Smad1-antisense oligomers showed much less expression of HSP47 and type IV collagen transcripts after AGE stimulation than those with control oligomers (Fig. 9).

DISCUSSION

This study shows that the collagen-specific chaperone protein, HSP47, is strongly expressed in glomerulosclerotic lesions in parallel with increased expression of collagens I and IV in diabetic nephropathy. The findings of the study also suggest that AGEs are a key factor in the synthesis of increased expression of both HSP47 and collagens *in vitro* and *in vivo*. Our *in vitro* study indicates that AGEs-mediated induction of HSP47 and collagens may be through TGF-β.

Collagen is synthesized in the form of pro-α chains, and three pro-α chains form procollagen with a triple-helical structure in the endoplasmic reticulum. HSP47 is a collagen-binding stress protein and has been shown to be localized exclusively in the endoplasmic reticulum. Procollagen polypeptides form a complex with HSP47 in the endoplasmic reticulum, which plays an important role as a collagen-specific molecular chaperone in the intracellular processing/folding of procollagen molecules (23, 24). The crucial role of HSP47 in regulating biosynthesis of collagen molecules has been reported previously (25), and transcriptional regulation for HSP47 expression was clarified (26, 27). However, its role in kidney diseases in relation to sclerosis/fibrosis in diabetic nephropathy and IgA nephropathy is completely unknown. We and others (8, 28) have demonstrated that HSP47 in glomerulosclerosis is associated with collagen staining. Furthermore, the blocking of HSP47 with antisense

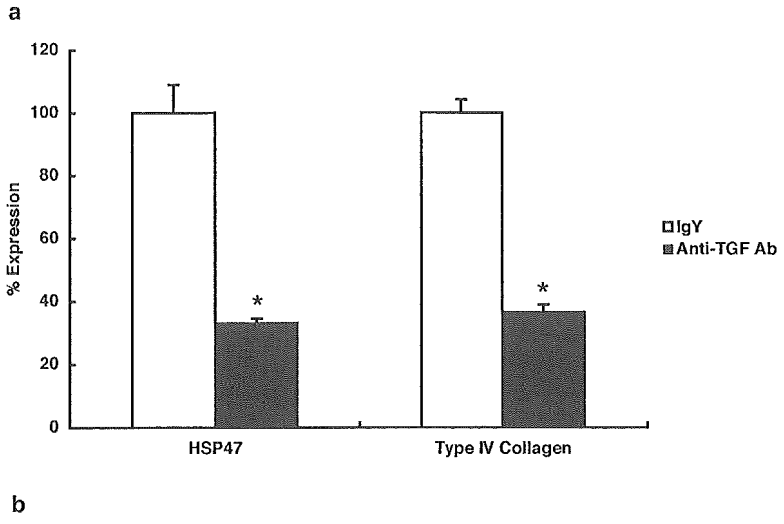

FIG. 7. **Inhibition of HSP47 and type IV collagen by TGF-β-neutralizing antibody.** *a*, neutralizing antibody for TGF-β inhibited both HSP47 and type IV collagen mRNA expressions in cultured mesangial cells (number of experiments, 5; *, $p < 0.05$ *versus* Control (IgY)). *b*, Western blot analysis of HSP47 and type IV collagen protein expression in cultured mesangial cells treated with AGE in the presence of neutralizing antibody for TGF-β or control (IgY).

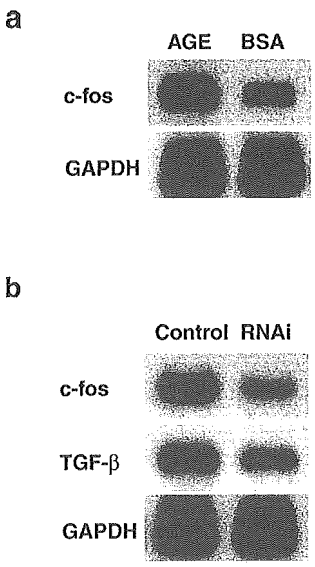

FIG. 8. **Regulation of c-*fos* mRNA expression by AGE.** *a*, RNase protection assay analysis of c-*fos* mRNA expression in total RNA lysates from cultured mesangial cells treated with AGE. One of three independent experiments is shown. *GAPDH* was used as an internal control. *b*, RNA interference (*RNAi*) against c-*fos* blocked the up-regulated mRNA level of *TGF-β* induced by AGE treatment. One of three independent experiments is shown.

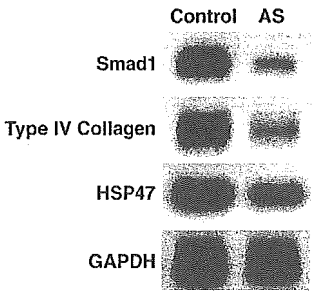

FIG. 9. **Effects of antisense oligomer specific for Smad1 in mesangial cells.** Antisense for *Smad1* (*AS*) blocked the up-regulated mRNA levels of *type IV collagen* and *HSP47* induced by AGE treatment on cultured mesangial cells. *Smad1* mismatch morpholino oligomer (*Control*) had no effect on the expression of these genes. One of three independent experiments is shown.

oligonucleotides caused a dramatic amelioration of glomerular lesions in the rat glomerulonephritis model (9). These findings suggest that HSP47 is a key factor in the development of various glomerular injuries. In this study, a close relationship of HSP47 to glomerulosclerosis in diabetic nephropathy was found.

The blocking of AGEs formation inhibited the overreproduction of HSP47 and collagens, thereby suppressing the gene expression of type IV collagen, extracellular matrix accumulation, and glomerulosclerosis in diabetic nephropathy *in vivo*. AGEs also increased mRNA expression of both HSP47 and type IV collagen *in vitro*. Thus, our study implicates that AGEs are a key factor in the synthesis of both HSP47 and collagens in diabetic nephropathy *in vivo* and *in vitro*. The mechanism of these processes remains unclarified, but we demonstrated that AGEs stimulate several novel transcription factors in gene expression for glomerulosclerosis (5). We have recently reported that Smad1 transcriptionally regulates of type IV collagen under AGE stimulation (14). Here, we also observed that the expression of HSP47 was regulated by Smad1 under AGE exposure. Yamamura *et al.* (29) has reported that TGF-β transcriptionally activates *HSP47* gene expression. Thus, Smad1 may partially participate in the TGF-β-mediated up-regulation of HSP47.

It has been shown that TGF-β stimulates the production of extracellular matrix components including collagens and fibronectin and that it plays a key role in glomerulosclerosis (12). TGF-β regulates the expression of the collagen genes and their transcriptional activities. In particular, the promoter analysis of the collagen genes revealed that TGF-β1 regulates the transcription of collagen genes via several *cis*-elements of their promoters (13). TGF-β also increases HSP47 gene expression in other cell types (29). We first demonstrated that TGF-β stimulates not only collagen but also HSP47 in mesangial cells. In addition, we showed that c-*Fos* participates in the induction of

TGF-β under AGE exposure. These data suggest that TGF-β and its signaling pathway are important targets for treating diabetic nephropathy.

Most experimental models of diabetic nephropathy are different from human pathological lesions (10, 30). On the other hand, the iNOSTg mice showed remarkably advanced glomerular lesions that resemble human diabetic glomerulosclerosis. From the analysis of this model, we confirmed that glomerular hypertrophy is important in the development of diabetic nephropathy because the iNOSTg mice showed glomerular hypertrophy in association with typical glomerulosclerosis. However, the intervention of AGE formation showed a decreased level of glomerulosclerosis with no evidence for diminished glomerular hypertrophy. The mechanism for this is unclear, but the regulation of HSP47 and collagens seemed to be independent of the control of glomerular hemodynamics. Further investigation will be needed to clarify the mechanism of these findings.

REFERENCES

1. Bojestig, M., Arnqvist, H. J., Hermansson, G., Karlberg, B. E., and Ludvigsson, J. (1994) *N. Engl. J. Med.* **330,** 15–18
2. Vlassara, H., Bucala, R., and Striker, L. (1994) *Lab. Investig.* **70,** 138–151
3. Yamamoto, Y., Kato, I., Doi, T., Yonekura, H., Ohashi, S., Takeuchi, M., Watanabe, T., Yamagishi, S., Sakurai, S., Takasawa, S., Okamoto, H., and Yamamoto, H. (2001) *J. Clin. Investig.* **108,** 261–268
4. Doi, T., Vlassara, H., Kirstein, M., Yamada, Y., Striker, G. E., and Striker, L. J. (1992) *Proc. Natl. Acad. Sci. U. S. A.* **89,** 2873–2877
5. Iehara, N., Takeoka, H., Yamada, Y., Kita, T., and Doi, T. (1996) *Kidney Int.* **50,** 1166–1172
6. Soulis-Liparota, T., Cooper, M., Papazoglou, D., Clarke, B., and Jerums, G. (1991) *Diabetes* **40,** 1328–1334
7. Nakamura, S., Makita, Z., Ishikawa, S., Yasumura, K., Fujii, W., Yanagisawa, K., Kawata, T., and Koike, T. (1997) *Diabetes* **46,** 895–899
8. Sunamoto, M., Kuze, K., Iehara, N., Takeoka, H., Nagata, K., Kita, T., and Doi, T. (1998) *Int. J. Exp. Pathol.* **79,** 133–140
9. Sunamoto, M., Kuze, K., Tsuji, H., Ohishi, N., Yagi, K., Nagata, K., Kita, T., and Doi, T. (1998) *Lab. Investig.* **78,** 967–972
10. Doi, T., Hattori, M., Agodoa, L. Y., Sato, T., Yoshida, H., Striker, L. J., and Striker, G. E. (1990) *Lab. Investig.* **63,** 204–212
11. Takamura, T., Kato, I., Kimura, N., Nakazawa, T., Yonekura, H., Takasawa, S., and Okamoto, H. (1998) *J. Biol. Chem.* **273,** 2493–2496
12. Border, W. A., and Ruoslahti, E. (1992) *J. Clin. Investig.* **90,** 1–7
13. Weigert, C., Brodbeck, K., Bierhaus, A., Haring, H. U., and Schleicher, E. D. (2003) *Biochem. Biophys. Res. Commun.* **304,** 301–307
14. Abe, H., Matsubara, T., Iehara, N., Nagai, K., Takahashi, T., Arai, H., Kita, T., and Doi, T. (2004) *J. Biol. Chem.* **279,** 14201–14206
15. Takeuchi, M., Makita, Z., Yanagisawa, K., Kameda, Y., and Koike, T. (1999) *Mol. Med.* **5,** 393–405
16. Doi, T., Striker, L. J., Gibson, C. C., Agodoa, L. Y., Brinster, R. L., and Striker, G. E. (1990) *Am. J. Pathol.* **137,** 541–552
17. Schutze, K., and Lahr, G. (1998) *Nat. Biotechnol.* **16,** 737–742
18. Fink, L., Seeger, W., Ermert, L., Hanze, J., Stahl, U., Grimminger, F., Kummer, W., and Bohle, R. M. (1998) *Nat. Med.* **4,** 1329–1333
19. Makibayashi, K., Tatematsu, M., Hirata, M., Fukushima, N., Kusano, K., Ohashi, S., Abe, H., Kuze, K., Fukatsu, A., Kita, T., and Doi, T. (2001) *Am. J. Pathol.* **158,** 1733–1741
20. MacKay, K., Striker, L. J., Elliot, S., Pinkert, C. A., Brinster, R. L., and Striker, G. E. (1988) *Kidney Int.* **33,** 677–684
21. Tsuji, H., Iehara, N., Masegi, T., Imura, M., Ohkawa, J., Arai, H., Ishii, K., Kita, T., and Doi, T. (1998) *Biochem. Biophys. Res. Commun.* **245,** 583–588
22. Abe, H., Iehara, N., Utsunomiya, K., Kita, T., and Doi, T. (1999) *J. Biol. Chem.* **274,** 20874–20878
23. Nagata, K., Saga, S., and Yamada, K. M. (1988) *Biochem. Biophys. Res. Commun.* **153,** 428–434
24. Nakai. A., Satoh, M., Hirayoshi, K., and Nagata, K. (1992) *J. Cell Biol.* **117,** 903–914
25. Nagai, N., Hosokawa, M., Itohara, S., Adachi, E., Matsushita, T., Hosokawa, N., and Nagata, K. (2000) *J. Cell Biol.* **150,** 1499–1506
26. Hirata, H., Yamamura, I., Yasuda, K., Kobayashi, A., Tada, N., Suzuki, M., Hirayoshi, K., Hosokawa, N., and Nagata, K. (1999) *J. Biol. Chem.* **274,** 35703–35710
27. Yasuda, K., Hirayoshi, K., Hirata, H., Kubota, H., Hosokawa, N., and Nagata, K. (2002) *J. Biol. Chem.* **277,** 44613–44622
28. Razzaque, M. S., Kumatori, A., Harada, T., and Taguchi, T. (1998) *Nephron* **80,** 434–443
29. Yamamura, I., Hirata, H., Hosokawa, N., and Nagata, K. (1998) *Biochem. Biophys. Res. Commun.* **244,** 68–74
30. Velasquez, M. T, Kimmel, P. L., and Michaelis, O. E., IV (1990) *FASEB J.* **4,** 2850–2859

MOLECULAR AND CELLULAR BIOLOGY, June 2004, p. 4627–4635 Vol. 24, No. 11
0270-7306/04/$08.00+0 DOI: 10.1128/MCB.24.11.4627–4635.2004

Role of *Hand1/eHAND* in the Dorso-Ventral Patterning and Interventricular Septum Formation in the Embryonic Heart

Kiyonori Togi,[1] Takahiro Kawamoto,[1] Ryoko Yamauchi,[2] Yoshinori Yoshida,[2] Toru Kita,[2] and Makoto Tanaka[1,3]*

Department of Geriatric Medicine[1] and Department of Cardiovascular Medicine,[2] Graduate School of Medicine, Kyoto University, and Department of Social Service, Kyoto University Hospital,[3] Kyoto, Japan

Received 18 November 2003/Returned for modification 17 December 2003/Accepted 25 February 2004

Molecular mechanisms for the dorso-ventral patterning and interventricular septum formation in the embryonic heart are unknown. To investigate a role of *Hand1/eHAND* in cardiac chamber formation, we generated *Hand1/eHAND* knock-in mice where *Hand1/eHAND* cDNA was placed under the control of the *MLC2V* promoter. In *Hand1/eHAND* knock-in mice, the outer curvature of the right and left ventricles expanded more markedly. Moreover, there was no interventricular groove or septum formation, although molecularly, *Hand1/eHAND* knock-in hearts had two ventricles. However, the morphology of the inner curvature of the ventricles, the atrioventricular canal, and the outflow tract was not affected by *Hand1/eHAND* expression. Furthermore, expression of *Hand1/eHAND* in the whole ventricles altered the expression patterns of *Chisel*, *ANF*, and *Hand2/dHAND* but did not affect *Tbx5* expression. In contrast, the interventricular septum formed normally in transgenic embryos overexpressing *Hand1/eHAND* in the right ventricle but not in the boundary region. These results suggested that *Hand1/eHAND* is involved in expansion of the ventricular walls and that absence of *Hand1/eHAND* expression in the boundary region between the right and left ventricles may be critical in the proper formation of the interventricular groove and septum. Furthermore, *Hand1/eHAND* is not a master regulatory gene that specifies the left ventricle myocyte lineage but may control the dorso-ventral patterning in concert with additional genes.

In vertebrate cardiac development, dorso-ventral (DV) patterning, as well as antero-posterior (AP) patterning, plays an essential role in the transformation of the linear heart tube into the four-chambered heart (7, 9). The linear heart tube is polarized along the AP axis, composed of five primordial segments: inflow tract (IFT), common atrium, atrioventricular canal (AVC), primitive ventricle, and outflow tract (OFT). Each segment is controlled by different developmental programs, characterized by specific gene expression profiles (2, 9, 20). In addition to the AP polarity, DV patterning has recently received attention. During cardiac looping, the ventricular chambers expand from the ventral surface of the heart tube (8). Trabeculae form only at the outer curvature of the heart tube, whereas the inner curvature remains smooth walled (7). Christoffels et al. and Lamers and Moorman proposed a two-step model for chamber formation in the embryonic heart (7, 13). First, the primary myocardium is induced, which makes up the linear heart tube. Second, the chamber myocardium is specified on the ventral side of the heart tube, acquiring an additional and presumably more advanced transcriptional program. In the looping heart, the specified chamber myocardium located at the outer curvature expands rapidly while the myocardium of the inner curvature, as well as the IFT, AVC, and OFT, retains the functional and molecular properties of the primary myocardium that has a limited proliferative capacity (7, 13). As a result, the atrial and ventricular chambers balloon out along the outer curvature (9). This ballooning model provides a view that DV, as well as AP, patterning information is critical for chamber specification. However, molecular mechanisms for the expansion of the chamber walls and the DV patterning of the embryonic heart are unknown.

Hand1/eHAND is a potential candidate gene. *Hand1/eHAND* is expressed on the ventral surface in the caudal half of the linear heart tube and predominantly at the outer curvature of the left ventricle (LV) in the looping heart while the gene is absent at the inner curvature (1, 21, 24). Therefore, its expression is highly restricted along the DV as well as the AP axis. Tetraploid-rescued *Hand1/eHAND* null embryos displayed a single ventricle, suggesting that the gene may play a critical role in specification or proliferation of LV myocytes during ballooning (17).

Moreover, the ballooning of chamber walls may be closely related to the formation of the interventricular septum (IVS). In the ballooning model, the structures flanking the atrial and ventricular chambers do not expand and retain the tubular shape, contributing to the proper AV septation and alignment of the IFT and OFT (7, 13). However, in this model, it is not clear what determines the boundary between the right ventricle (RV) and LV. The myocardium at the interventricular groove (IVG) is not the primary but working myocardium according to this model, but this region does not expand. It is totally unknown what molecular mechanisms determine the location of the IVS and IVG.

In this study, we examined a role of *Hand1/eHAND* in the DV patterning of the embryonic heart and the IVS formation. For this purpose, we knocked in the *Hand1/eHAND* gene to

* Corresponding author. Mailing address: Department of Social Service, Kyoto University Hospital, 54 Shogoin-Kawahara-cho, Sakyo-ku, Kyoto 606-8507, Japan. Phone: 81-75-751-3465. Fax: 81-75-751-3574. E-mail: makoto@kuhp.kyoto-u.ac.jp.